Stationary nonequilibrium bound state of a pair of run and tumble particles

Pierre Le Doussal,[1] Satya N. Majumdar,[2] and Grégory Schehr[3]
[1]*CNRS-Laboratoire de Physique Théorique de l'Ecole Normale Supérieure, 24 rue Lhomond, 75231 Paris Cedex, France*
[2]*Université Paris-Saclay, CNRS, LPTMS, 91405, Orsay, France*
[3]*Sorbonne Université, Laboratoire de Physique Théorique et Hautes Energies, CNRS UMR 7589, 4 Place Jussieu, 75252 Paris Cedex 05, France*

(Received 1 June 2021; accepted 9 September 2021; published 4 October 2021)

We study two interacting identical run-and-tumble particles (RTPs) in one dimension. Each particle is driven by a telegraphic noise and, in some cases, also subjected to a thermal white noise with a corresponding diffusion constant D. We are interested in the stationary bound state formed by the two RTPs in the presence of a mutual attractive interaction. The distribution of the relative coordinate y indeed reaches a steady state that we characterize in terms of the solution of a second-order differential equation. We obtain the explicit formula for the stationary probability $P(y)$ of y for two examples of interaction potential $V(y)$. The first one corresponds to $V(y) \sim |y|$. In this case, for $D = 0$ we find that $P(y)$ contains a δ function part at $y = 0$, signaling a strong clustering effect, together with a smooth exponential component. For $D > 0$, the δ function part broadens, leading instead to weak clustering. The second example is the harmonic attraction $V(y) \sim y^2$ in which case, for $D = 0$, $P(y)$ is supported on a finite interval. We unveil an interesting relation between this two-RTP model with harmonic attraction and a three-state single-RTP model in one dimension, as well as with a four-state single-RTP model in two dimensions. We also provide a general discussion of the stationary bound state, including examples where it is not unique, e.g., when the particles cannot cross due to an additional short-range repulsion.

DOI: 10.1103/PhysRevE.104.044103

I. INTRODUCTION

Interacting active particles is a subject of much current interest both theoretically and experimentally [1–7]. An active particle, in contrast to a passive particle, has an autonomous self-propelled motion, which is modeled by a driving "active" noise, which has a finite persistence time. For example, a commonly studied model is the so-called run-and-tumble particle (RTP)—a motion exhibited by *Escherichia coli* bacteria [5,7]. In this simplest RTP model, the particle chooses a direction at random and moves ballistically with a constant speed v_0 in that direction during an exponentially distributed random run time with mean γ^{-1}. Then it tumbles, i.e., it changes its direction at random and again moves ballistically with speed v_0, performing a new run. Thus, runs and tumbles alternate. The tumbling rate γ and the speed v_0 are the two parameters in this simplest RTP model. For example, in one dimension, the position $x(t)$ of the RTP evolves via the stochastic equation

$$\frac{dx(t)}{dt} = v_0\,\sigma(t), \tag{1}$$

where $\sigma(t)$ is a telegraphic noise that takes values $\sigma(t) = \pm 1$ and changes from one state to another with a constant rate γ. Thus, this "active noise" $\sigma(t)$ has zero mean $\langle \sigma(t) \rangle = 0$ and its auto-correlation function decays exponentially in time $\langle \sigma(t)\sigma(t') \rangle = e^{-2\gamma\,|t-t'|}$. Therefore, the active process $x(t)$ is non-Markovian since the driving noise has a finite memory characterized by the persistence time γ^{-1}. In fact, much before the current interest in the context of active matter, this RTP model in one-dimension has been studied extensively both in the mathematics and the physics literature where it is known as "persistent" random walk [8–12]. In the limit $\gamma \to \infty$, the active noise reduces to a "passive" δ-correlated noise. At long times, the effect of activity becomes somewhat insignificant since a free RTP is known to converge to a Brownian motion with an effective diffusion constant $D_{\rm eff} = v_0^2/(2\gamma)$. Thus, the presence of activity is detected only in the effective diffusion constant $D_{\rm eff}$. One can also add a thermal noise in Eq. (1),

$$\frac{dx(t)}{dt} = v_0\,\sigma(t) + \sqrt{2D}\xi(t), \tag{2}$$

where $\xi(t)$ is a Gaussian white noise with zero mean and a correlator $\langle \xi(t)\xi(t') \rangle = \delta(t - t')$. Here also the system becomes diffusive at late times with an effective diffusion constant $D_{\rm eff} = v_0^2/(2\gamma) + D$ [2,13]. Thus, the effect of an additional thermal noise, in this simple setting, is just to renormalize the effective diffusion constant at late times.

There are two natural generalizations of this single-free-RTP dynamics described above in Eq. (1). The first concerns the long-time stationary state of the RTP in the presence of an external confining potential. In this case, the evolution Eq. (2) has an additional external force $F(x) = -U'(x)$, with $U(x)$ being the confining potential,

$$\frac{dx(t)}{dt} = F(x) + v_0\,\sigma(t) + \sqrt{2D}\xi(t). \tag{3}$$

Here, at late times, the system reaches a stationary state which is typically non-Boltzmann, thus retaining the effect of activity even at late times [11,14–20]. The second generalization is to study several RTPs with pairwise interactions (repulsive or

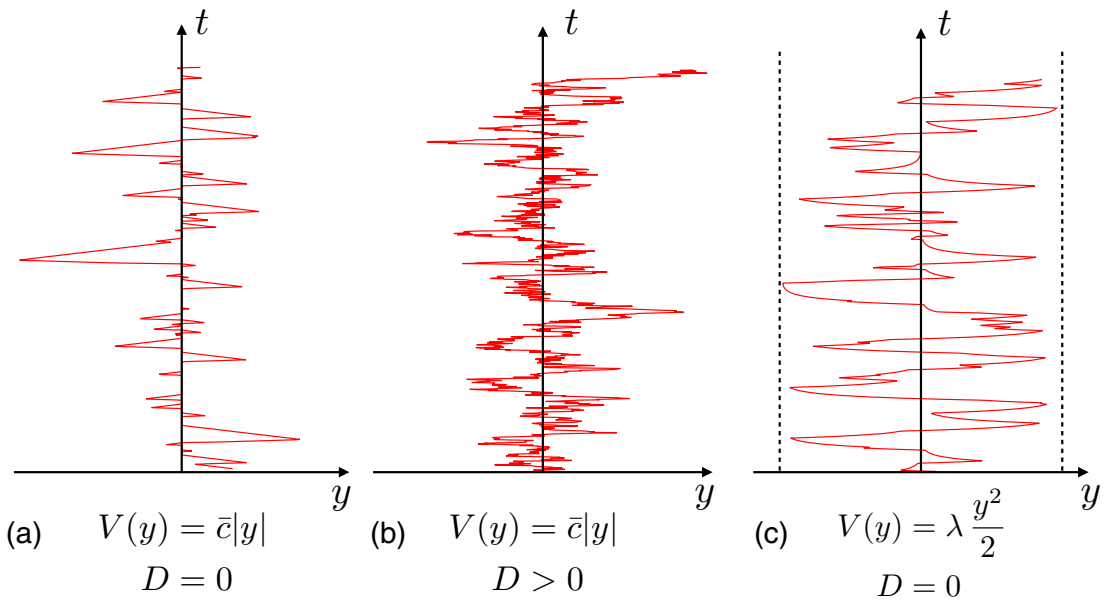

FIG. 1. Typical trajectories of the relative coordinate y as a function of time t [obtained by solving numerically the equation of motion Eq. (6)] for the three different models for which we compute here exactly the stationary distribution $P(y, t \to \infty)$: (a) $V(y) = \bar{c}|y|$ with $D = 0$, (b) $V(y) = \bar{c}|y|$ with $D > 0$, and (c) $V(y) = \lambda y^2/2$ with $D = 0$. In case (a), the system exhibits strong clustering characterized by the presence of a δ function at $y = 0$ in the steady state [see Eq. (32)] and clearly seen on the figure where y sticks to zero from time to time, while in case (b) the system exhibits only weak clustering since the thermal noise (i.e., $D > 0$) broadens the δ function [see Eq. (60)]. Finally, in case (c), the relative coordinate y is bounded in the steady state, as indicated by the vertical dotted lines [see, e.g., Eq. (97)].

attractive) between them. In the presence of interactions, RTPs are known to exhibit interesting collective effects, such as clustering and jamming [1,3,7,21,22]. While there have been several studies on the effect of interactions between RTPs, there still are very few exact results available. For example, even for two RTPs on a ring with hard-core repulsion between them, the steady state exhibits clustering and the solution is nontrivial [21–24]. Note that with repulsive interactions between the RTPs, the steady state will exist only in a finite size system. In an infinite system with two particles, while there is no steady state, other dynamical properties have been studied—for example, the probability that two particles do not cross each other up to time t has been computed exactly and it was shown to be already nontrivial due to the presence of the active noise [25].

To obtain a steady state for a system of RTPs in an infinite system (in the frame of the center of mass), one needs to introduce an attractive interaction between the RTPs. For instance, in the simplest setting of two particles with attractive interactions between them, one would expect to see clustering in the steady state in the form of a bound pair. The stationary properties of such bound pairs, even in an infinite system, are difficult to describe analytically. In fact, there are hardly any analytical results available in the literature on such bound pairs.

In this paper, we study a simple model of two RTPs on an infinite line with attractive interaction between them. We provide exact analytical results for the steady-state distribution of the interparticle distance for different types of attractive interactions. These results provide a complete characterization of the bound pair. Even though our system is extremely simple, it turns out that the stationary state of the bound pair has a very rich structure which depends on the shape of the interaction. In some cases, e.g., for a linear interaction potential, and when the particles are driven purely by active noise [see Fig. 1(a)], one finds that the clustering is "strong," a signature of which is the presence of a Dirac δ function in the steady-state distribution of the interparticle distance. In that case, adding the thermal noise broadens the δ function, indicating a "weak" clustering [see Fig. 1(b)], with exponential decay of the steady-state distribution of the interparticle distance. In other cases, e.g., for a harmonic interaction potential, the interparticle distance in the steady state remains bounded in a finite interval [see Fig. 1(c)].

The rest of the paper is organized as follows. In Sec. II, we introduce precisely our model and summarize the main results. In Sec. III, we focus on the special case of a linear attractive potential $V(y) = \bar{c}|y|$ for which we compute exactly the stationary state, both in the absence (Sec. III A) and in the presence (Sec. III B) of the thermal noise. In Sec. IV, we study the case of a general $V(y)$, but in the absence of thermal noise. Finally, we conclude in Sec. V.

II. THE MODEL AND A SUMMARY OF THE RESULTS

In this paper, we consider two interacting RTPs on the line described by the equation of motion

$$\begin{aligned} \frac{dx_1}{dt} &= f(x_1 - x_2) + v_0\,\sigma_1(t) + \sqrt{2D}\,\xi_1(t), \\ \frac{dx_2}{dt} &= f(x_2 - x_1) + v_0\sigma_2(t) + \sqrt{2D}\,\xi_2(t), \\ f(-y) &= -f(y), \end{aligned} \tag{4}$$

where $\sigma_1(t) = \pm 1$ and $\sigma_2(t) = \pm 1$ are two independent telegraphic noises with flipping rate γ. In addition, both particles

are also driven by thermal noises, represented by independent Gaussian white noises $\xi_1(t)$ and $\xi_2(t)$ of zero mean and correlators $\langle \xi_i(t)\xi_j(t')\rangle = \delta_{ij}\delta(t-t')$. We assume that both of them have the same diffusion constant D. The two RTPs interact via a potential energy $V(x_1 - x_2)$ and in Eq. (4) $f(y) = -V'(y)$ is the interparticle force. Equivalently, denoting $w = (x_1 + x_2)/2$ and $y = x_1 - x_2$, one has

$$\frac{dw}{dt} = \frac{v_0}{2}\,[\sigma_1(t) + \sigma_2(t)] + \sqrt{D}\,\tilde{\eta}(t), \tag{5}$$

$$\frac{dy}{dt} = 2f(y) + v_0\,[\sigma_1(t) - \sigma_2(t)] + \sqrt{4D}\,\eta(t), \tag{6}$$

where $\eta(t) = [\xi_1(t) - \xi_2(t)]/\sqrt{2}$ and $\tilde{\eta}(t) = [\xi_1(t) + \xi_2(t)]/\sqrt{2}$ are two independent Gaussian white noises with zero mean, each with a δ-correlator. The center of mass w undergoes a free RTP motion similar to Eq. (2) and clearly does not reach a stationary state. Hence, we will focus here only on the relative coordinate $y(t)$ which evolves independently of $w(t)$. In other words we study the system in the center of mass frame. By comparing Eqs. (3) and (6), we see that the dynamics of the relative coordinate $y(t)$ in Eq. (6) can be interpreted as the dynamics of the position of a single RTP with three internal states $(-2v_0, 0, 2v_0)$, and subjected to an external force $2f(y)$. If $f(y)$ is sufficiently attractive, then we expect that the relative coordinate will reach a stationary state, leading to a stationary bound state of the pair of particles. Denoting by $P(y,t)$ the distribution of the relative coordinate at time t, our goal is to evaluate its stationary limit $P(y, t \to \infty)$. Note that the only difference between Eqs. (3) and (6) is that the driving active noise in the former case has two states, while in the latter it has three states. In the former case, Eq. (3), the stationary position distribution for arbitrary $f(y)$ is exactly known, at least for $D = 0$. In contrast, when the driving active noise has three states, as in Eq. (6), it is more difficult to compute the stationary distribution of the relative coordinate for arbitrary $f(y)$, even for $D = 0$. In this paper we derive a second-order differential equation, see Eq. (84), which is obeyed by this stationary distribution $P(y, t \to \infty)$. It is challenging to solve it analytically for a general $f(y)$, but here we obtain explicit solutions for two special cases of $f(y)$ as discussed below.

To compute the stationary state, we start from the Langevin Eq. (6) for the relative coordinate $y(t)$, and write down the corresponding Fokker-Planck (FP) equation. However, due to the finite memory of the active noises $\sigma_1(t)$ and $\sigma_2(t)$, the process is Markov only when one keeps track of the two internal degrees of freedom $\sigma_1(t)$ and $\sigma_2(t)$, in addition to $y(t)$. This obliges us to define $P_{\sigma_1,\sigma_2}(y,t)$ as the joint probability density for the relative coordinate to be at y at time t and that the internal "spins" $\sigma_1(t)$ and $\sigma_2(t)$ take values σ_1 and σ_2 at time t. One can then write down the four coupled FP equations for $P_{\sigma_1,\sigma_2}(y,t)$ corresponding to $\sigma_1 = \pm 1$ and $\sigma_2 = \pm 1$. The distribution of the relative coordinate $P(y,t)$ is then obtained by summing over the four internal states,

$$P(y,t) = \sum_{\sigma_1=\pm1,\sigma_2=\pm1} P_{\sigma_1,\sigma_2}(y,t). \tag{7}$$

However, for general $f(y)$, solving these FP equations, even in the stationary state, turns out to be rather hard. There is however one special case, namely, when $V(y) = \bar{c}\,|y|$ [corresponding to $f(y) = -\bar{c}\,\mathrm{sgn}(y)$], for which one can obtain the stationary state explicitly for arbitrary $D \geqslant 0$. We present this solution in detail in Sec. III, first in the absence of the thermal noise ($D = 0$) and then in the presence of the thermal noise $D > 0$. This allows us investigate the effect of thermal noise on the stationary state. Our main result is that, when $D = 0$, the stationary state $P(y, t \to \infty)$ has two parts: (i) an exponentially decaying part and (ii) a δ function at $y = 0$ [see Eqs. (31) and (35)]. As mentioned above, the presence of this δ function is a signature of *strong* clustering. When $D > 0$ is switched on, the δ-function part gets smeared and the stationary state consists only of decaying exponentials [see for instance Eq. (60)]. Thus, the effect of the thermal noise in the stationary state is to weaken the clustering. The second case for which we find an explicit solution is the harmonic potential $V(y) = \lambda y^2/2$, which we study only for $D = 0$. In that case, the support of the stationary distribution of the relative coordinate is a single interval, where $P(y)$ exhibits some power-law singular behavior near the edges and at the center $y = 0$, with exponents depending on the parameters γ and λ. It turns out that in this harmonic case the stationary solution is identical to the solution of another three-state model that was studied recently [19], even though the dynamics of the two models are quite different. In the presence of a $D > 0$, although we did not study it, we expect the support to extend to the full real axis.

Before proceeding to the technical details, let us briefly comment on the possible physical realizations of the model in Eq. (6). As discussed above, in Eq. (6), the relative coordinate y can be interpreted as the position of a single RTP subjected to an external confining potential $2V(y)$ and with three internal states $(-2v_0, 0, 2v_0)$ for the driving telegraphic noise, as well as a diffusive noise $\sqrt{4D}\,\eta(t)$. The external confining potential and the ensuing attractive force towards $y = 0$ mimics the presence of a nutrient gradient for the RTP, e.g., as for an *E. coli* bacteria searching for food. The only difference, in this model, from the standard RTP is that the bacteria has three velocity states. In particular the state $v = 0$ is the new one. This has the following interpretation. When the internal state v is zero, the particle is at rest (but still with a diffusive noise). This may mimic a local diffusive search by a bacteria, before it switches to positive or negative velocities to explore a larger region. This is thus similar to intermittent search strategies commonly employed by various animals during their foraging period [26].

Another interpretation of Eq. (6) for the special case where $f(y) = -\bar{c}\,\mathrm{sgn}(y)$ where $\mathrm{sgn}(y)$ is the sign function, is that it can be considered as a generalized active version of the so-called "dry-friction" model introduced by de Gennes [27] and subsequently studied by others [28–30].

III. STATIONARY SOLUTION FOR THE LINEAR INTERACTION POTENTIAL

In this section we will study the stationary state of the interparticle distance $y(t)$ in the presence of an attractive potential $V(y) = \bar{c}|y|$, with $\bar{c} > 0$ (similar to the Coulomb interaction between two opposite charges in one dimension). This corresponds to a force $f(y) = -V'(y) = -\bar{c}\,\mathrm{sgn}(y)$. In

this case, the evolution equation for $y(t)$ in Eq. (6) reads

$$\frac{dy}{dt} = -2\bar{c}\,\mathrm{sgn}(y) + v_0\,[\sigma_1(t) - \sigma_2(t)] + \sqrt{4D}\,\eta(t). \quad (8)$$

In general, for arbitrary $f(y)$ in Eq. (6), it is not easy to compute the stationary state in the presence of the thermal noise ($D > 0$). However, in this special case when $f(y) = -\bar{c}\,\mathrm{sgn}(y)$, we show below that the stationary state for $y(t)$ can be fully characterized, both for $D = 0$ and for $D > 0$.

A. Without thermal noise, $D = 0$

In this subsection we study the process in Eq. (8) in the absence of thermal noise $D = 0$. We note that $y(t)$ in Eq. (8) is actually a non-Markov process, since $\sigma_1(t)$ and $\sigma_2(t)$ have a finite memory. To write a FP equation, we need to recast first the dynamics into a Markovian form. This is usually done by enlarging the phase space—here, e.g., by considering the evolution of the triplet $\{y(t), \sigma_1(t), \sigma_2(t)\}$. This leads us to define $P_{\sigma_1,\sigma_2}(y,t)$ as the joint probability density function (PDF) that at time t, the relative coordinate takes the value y and the internal states take values σ_1 and σ_2, respectively. To obtain the time evolution of this PDF, we evolve the system from time t to $t + \Delta t$, with $\Delta t \ll 1$, and consider the changes (loss and gain) in $P_{\sigma_1,\sigma_2}(y,t)$. By keeping terms up to order $O(\Delta t)$, we get the following FP equation:

$$\partial_t P_{\sigma_1,\sigma_2} = -\partial_y\big\{[-2\bar{c}\,\mathrm{sgn}(y) + v_0(\sigma_1 - \sigma_2)]P_{\sigma_1,\sigma_2}\big\} - 2\gamma P_{\sigma_1,\sigma_2} + \gamma\big(P_{-\sigma_1,\sigma_2} + P_{\sigma_1,-\sigma_2}\big). \quad (9)$$

In Eq. (9), σ_1 and σ_2 can both take values ± 1 and we recall that γ is the rate at which the telegraphic noises $\sigma_1(t)$ and $\sigma_2(t)$ change signs. In Eq. (9) the first term on the right-hand side (r.h.s.) describes the standard advection due to the drift term in the Langevin Eq. (8), while the second and the third terms describe, respectively, the loss and gain by flipping one of the σ_i's. Note that on the r.h.s. there is no term involving $P_{-\sigma_1,-\sigma_2}$. This is because to arrive at (σ_1,σ_2) from $(-\sigma_1,-\sigma_2)$ would involve a simultaneous flipping of both σ_1 and σ_2 whose probability is $\gamma^2\Delta t^2$. Hence, Eq. (9) describes actually four coupled equations depending on the four values of $\{\sigma_1,\sigma_2\}$, namely, $P_{++}(y,t)$, $P_{+-}(y,t)$, $P_{-+}(y,t)$ and $P_{--}(y,t)$. The first term on the r.h.s. of Eq. (9) describes the convection in the presence of an external force, while the rest of the terms denote the loss and gain due to the flipping of the telegraphic noise. The total probability $P(y,t)$ is then obtained by summing over the internal degrees of freedom as in Eq. (7).

Before analyzing the FP Eq. (9) let us investigate the Langevin equation and see what we may anticipate for the evolution of the system. It reads

$$\frac{dy}{dt} = -2\,\bar{c}\,\mathrm{sgn}(y) + v_0\,[\sigma_1(t) - \sigma_2(t)]. \quad (10)$$

Consider for instance the case when $[\sigma_1(t),\sigma_2(t)]$ are either $(+,+)$ or $(-,-)$, in which case $\frac{dy}{dt} = -2\bar{c}\,\mathrm{sgn}(y)$. Therefore, for $y(0) > 0$ the time evolution is $y(t) = y(0) - 2\bar{c}t$ and $y(t)$ vanishes in finite time. At all later times it remains zero until one of the $\sigma_i(t)$ changes sign provided $v_0 > \bar{c}$. This is a clustering effect which will lead to the appearance of a δ-function component, $\propto \delta(y)$ in $P_{\sigma_1,\sigma_2}(y,t)$. In fact, when $v_0 < \bar{c}$ we expect that the total probability $P(y,t)$ converges to $\delta(y)$ in finite time and remains there. In contrast, for $v_0 > \bar{c}$ we expect a non trivial stationary distribution, where the δ function at $y = 0$ coexists with a continuous background.

We expect the system to reach a stationary state in the long time limit $t \to \infty$. For simplicity of notations, we will denote the stationary state by $P_{\sigma_1,\sigma_2}(y) = P_{\sigma_1,\sigma_2}(y, t \to \infty)$. The stationary solution can be obtained from Eq. (9) by setting $\partial_t P_{\sigma_1,\sigma_2} = 0$ in the left-hand side (l.h.s.) of Eq. (9). This leads to

$$0 = -\partial_y\big\{[-2\bar{c}\,\mathrm{sgn}(y) + v_0(\sigma_1 - \sigma_2)]P_{\sigma_1,\sigma_2}\big\} - 2\gamma P_{\sigma_1,\sigma_2} + \gamma\big(P_{-\sigma_1,\sigma_2} + P_{\sigma_1,-\sigma_2}\big). \quad (11)$$

Since up to the sign of y the equation is linear with constant coefficients, it is natural to look for exponential solutions. In addition, as discussed below Eq. (10), we anticipate also the presence of a δ function at $y = 0$. This leads us to look for a solution of the form

$$P_{\sigma_1,\sigma_2}(y) = A^{\epsilon}_{\sigma_1,\sigma_2} e^{-\mu|y|} + B_{\sigma_1,\sigma_2}\delta(y), \quad (12)$$

where $\mu > 0$ (to be fixed later) and $\epsilon = \mathrm{sgn}(y)$. For a given σ_1,σ_2, there is no reason *a priori*, that the solution $P_{\sigma_1,\sigma_2}(y)$ is symmetric around $y = 0$, even though the potential $V(y) = \bar{c}|y|$ is symmetric around $y = 0$. This is because the dynamics of y also depends explicitly on σ_1 and σ_2, and not just on y alone. Hence, we put different sets of constants in front of the exponentials in Eq. (12) for $y > 0$ and $y < 0$ and they are denoted by different vectors $A^{+}_{\sigma_1,\sigma_2}$ and $A^{-}_{\sigma_1,\sigma_2}$. Note that each of them is a four-component column vector; hence, we have eight different unknown constants. However, they are related via the symmetry relations $A^{+}_{\sigma_1,\sigma_2} = A^{-}_{\sigma_2,\sigma_1}$. This follows from the fact that Eq. (9) is invariant under the simultaneous change $y \to -y$ and $(\sigma_1,\sigma_2) \to (\sigma_2,\sigma_1)$. Hence, it suffices to know for instance just the vector A^{+}, which has thus four unknown constants. In addition, the amplitudes of the δ function defined in Eq. (12) also form a four-component column vector, with four additional unknown constants. Therefore, in total, we have eight constants to determine.

By analyzing Eq. (11) around $y = 0$, we arrive at two types of conditions. The first one is that upon injecting the form of Eq. (12) in Eq. (11) there should be no term generated proportional to $\delta'(y)$ which implies that for any σ_1,σ_2,

$$(\sigma_1 - \sigma_2)B_{\sigma_1,\sigma_2} = 0. \quad (13)$$

As a consequence we obtain $B_{+-} = B_{-+} = 0$. In addition, due to the symmetry $y \to -y$ and $(\sigma_1,\sigma_2) \to (-\sigma_1,-\sigma_2)$ we expect that $B_{++} = B_{--}$. Summarizing,

$$B_{+-} = B_{-+} = 0, \quad B_{++} = B_{--}. \quad (14)$$

Hence, for the vector B, we have only one unknown constant to determine. Combining A^{ϵ} (with $\epsilon = \pm 1$) and B, we then have a total of five unknown constants to determine. Hence, we need five relations to fix them. One of them is provided by the normalization condition, namely, $\int_{-\infty}^{\infty} P(y)\,dy = 1$. The rest of the four conditions can be derived by integrating the FP Eqs. (11) over a small region across $y = 0$. This reads

$$\big\{[2\bar{c}\,\mathrm{sgn}(y) - v_0(\sigma_1 - \sigma_2)]P_{\sigma_1,\sigma_2}\big\}_{0^-}^{0^+} - 2\gamma B_{\sigma_1,\sigma_2} + \gamma\big(B_{-\sigma_1,\sigma_2} + B_{\sigma_1,-\sigma_2}\big) = 0, \quad (15)$$

where the second term comes from the contribution of the δ function in Eq. (12). Evaluating the first term gives

$$\begin{aligned}&\left\{[2\bar{c}\,\mathrm{sgn}(y)-v_0(\sigma_1-\sigma_2)]P_{\sigma_1,\sigma_2}\right\}_{0^-}^{0^+}\\&\quad=2\bar{c}\left(A^+_{\sigma_1,\sigma_2}+A^-_{\sigma_1,\sigma_2}\right)-v_0(\sigma_1-\sigma_2)\left(A^+_{\sigma_1,\sigma_2}-A^-_{\sigma_1,\sigma_2}\right).\end{aligned}\tag{16}$$

Substituting Eq. (16) in Eq. (15) gives us the four required conditions, namely,

$$\begin{aligned}&2\bar{c}\left(A^+_{\sigma_1,\sigma_2}+A^-_{\sigma_1,\sigma_2}\right)-v_0(\sigma_1-\sigma_2)\left(A^+_{\sigma_1,\sigma_2}-A^-_{\sigma_1,\sigma_2}\right)\\&\quad-2\gamma B_{\sigma_1,\sigma_2}+\gamma\left(B_{-\sigma_1,\sigma_2}+B_{\sigma_1,-\sigma_2}\right)=0,\end{aligned}\tag{17}$$

for $\sigma_1=\pm1$ and $\sigma_2=\pm1$. These four conditions Eq. (17) in addition to the normalization condition provide us exactly five relations to determine the five unknown constants. In addition, we need to determine the value of μ, to which we now turn to.

To determine μ, we insert Eq. (12) in Eq. (11) in the stationary state and find that the amplitude vector A^ϵ must satisfy

$$\mathcal{M}_\epsilon(\mu)\cdot\begin{pmatrix}A^\epsilon_{++}\\A^\epsilon_{+-}\\A^\epsilon_{-+}\\A^\epsilon_{--}\end{pmatrix}=0,\tag{18}$$

where we have defined the 4×4 matrices $\mathcal{M}_\pm(\mu)$ as

$$\begin{aligned}\mathcal{M}_\epsilon(\mu)&=(-2\mu\bar{c}-2\gamma)\,\mathbb{I}+M(\epsilon\mu),\\M(\mu)&=\begin{pmatrix}0&\gamma&\gamma&0\\\gamma&2\mu v_0&0&\gamma\\\gamma&0&-2\mu v_0&\gamma\\0&\gamma&\gamma&0\end{pmatrix}.\end{aligned}\tag{19}$$

The relations in Eq. (18) provide a set of four linear equations for the $A^\epsilon_{\sigma_1,\sigma_2}$. The solutions for the $A^\epsilon_{\sigma_1,\sigma_2}$ are identically zero, unless the determinant of $\mathcal{M}_\epsilon(\mu)$ vanishes. This condition that $\det\mathcal{M}_\epsilon(\mu)=0$ actually fixes the value of μ. To compute the determinant, we need to evalute the eigenvalues of $\mathcal{M}_\epsilon(\mu)$, which thanks to Eq. (19), amounts to computing the eigenvalues of the matrix $M(\mu)$. They are given by

$$\left(0,0,-2\sqrt{\gamma^2+\mu^2v_0^2},\;2\sqrt{\gamma^2+\mu^2v_0^2}\right),\tag{20}$$

and the associated eigenvectors are given by the columns of the 4×4 matrix $\hat{O}$,

$$\begin{aligned}\hat{O}&=\begin{pmatrix}-\frac{1}{\sqrt2}&\frac{c}{\sqrt2}&\frac{s}{2}&\frac{s}{2}\\0&\frac{s}{\sqrt2}&-\frac12(1+c)&\frac12(1-c)\\0&-\frac{s}{\sqrt2}&-\frac12(1-c)&\frac12(1+c)\\\frac{1}{\sqrt2}&\frac{c}{\sqrt2}&\frac{s}{2}&\frac{s}{2}\end{pmatrix},\\c&=\frac{-\mu v_0}{\sqrt{\gamma^2+\mu^2v_0^2}},\quad s=\frac{\gamma}{\sqrt{\gamma^2+\mu^2v_0^2}},\end{aligned}\tag{21}$$

with $c^2+s^2=1$. We will denote the four column vectors, respectively, by $(V^1,V^2(\mu),V^3(\mu),V^4(\mu))$. Each of the V^α with $\alpha=1,2,3,4$ is a four-column vector and they form an orthonormal basis. Hence, we get

$$\begin{aligned}\det\mathcal{M}_\epsilon(\mu)=(-2\mu\bar{c}-2\gamma)^2\left(-2\mu\bar{c}-2\gamma-2\sqrt{\gamma^2+\mu^2v_0^2}\right)\\\times\left(-2\mu\bar{c}-2\gamma+2\sqrt{\gamma^2+\mu^2v_0^2}\right)=0.\end{aligned}\tag{22}$$

We can obtain different solutions for μ by setting each of the factors [corresponding to four different eigenvalues of $\mathcal{M}_\epsilon(\mu)$] to zero. However, it turns out that only the last eigenvalue [corresponding to the last factor in Eq. (22)] gives a real positive solution for μ which reads

$$\mu=\mu^*=\frac{2\bar{c}\gamma}{v_0^2-\bar{c}^2},\tag{23}$$

where we recall that we are studying the case $v_0>\bar{c}$, such that there is a bound state, i.e., where the distribution is localized in space (exponentially decaying tail). The solution for A^ϵ, corresponding to this fourth eigenvalue is therefore $A^\epsilon\propto V^4(\epsilon\mu)$, i.e.,

$$\begin{aligned}A^\epsilon_{\sigma_1,\sigma_2}&=aV^4_{\sigma_1,\sigma_2}(\epsilon\mu^*)=a\begin{pmatrix}\frac{s}{2}\\\frac12(1-\epsilon c)\\\frac12(1+\epsilon c)\\\frac{s}{2}\end{pmatrix},\\c&=\frac{-\mu^*v_0}{\sqrt{\gamma^2+(\mu^*)^2v_0^2}}=\frac{-2v_0\bar{c}}{v_0^2+\bar{c}^2},\\s&=\frac{\gamma}{\sqrt{\gamma^2+(\mu^*)^2v_0^2}}=\frac{v_0^2-\bar{c}^2}{v_0^2+\bar{c}^2},\end{aligned}\tag{24}$$

where a is an *a priori* unknown amplitude determined below, and c and s are given in Eq. (21) with μ^* given in Eq. (23). Note that the symmetry $A^\epsilon_{\sigma_1,\sigma_2}=A^{-\epsilon}_{\sigma_2,\sigma_1}$ discussed above implies that a does not depend on ϵ. This is because, under this symmetry, the eigenvector $V^4_{\sigma_1,\sigma_2}(\epsilon\mu^*)$ in Eq. (24) remains invariant, hence a cannot depend on ϵ. Thus, we have reduced the problem of determining 4 unknown constants in the column-vector $A^+_{\sigma_1,\sigma_2}$ to the problem of determining just one constant a. Thus, to summarize, at this stage, we have two unknowns a and B_{++} to determine. To proceed, we first rewrite the condition Eq. (17) explicitly,

$$\begin{aligned}&2\bar{c}a\begin{pmatrix}s\\1\\1\\s\end{pmatrix}+v_0a\begin{pmatrix}0\\2c\\2c\\0\end{pmatrix}\\&\quad+\begin{pmatrix}-2\gamma&\gamma&\gamma&0\\\gamma&-2\gamma&0&\gamma\\\gamma&0&-2\gamma&\gamma\\0&\gamma&\gamma&-2\gamma\end{pmatrix}\begin{pmatrix}B_{++}\\B_{+-}\\B_{-+}\\B_{--}\end{pmatrix}=0.\end{aligned}\tag{25}$$

Next, we use Eq. (14) to eliminate B_{+-}, B_{-+}, and B_{--} in favour of B_{++}. This gives the two relations

$$2a\bar{c}s-2\gamma B_{++}=0,\tag{26}$$

$$2a(\bar{c}+v_0c)+2\gamma B_{++}=0,\tag{27}$$

which are actually equivalent using the values for c and s from Eq. (24). This leads to the single relation

$$B_{++} = a\,\bar{c}\,\frac{v_0^2 - \bar{c}^2}{\gamma\left(v_0^2 + \bar{c}^2\right)}. \tag{28}$$

We are then left with one unknown constant a to determine and this will be fixed by the normalization condition. Injecting these results in the form of Eq. (12) and summing over σ_1, σ_2 we obtain the total probability

$$P(y) = \sum_{\sigma_1=\pm1,\sigma_2=\pm1} P_{\sigma_1,\sigma_2}(y) = a(s+1)e^{-\mu^*|y|} + 2B_{++}\delta(y)$$
$$= 2a\left[\frac{v_0^2}{v_0^2+\bar{c}^2}e^{-\mu|y|} + \bar{c}\,\frac{v_0^2-\bar{c}^2}{\gamma\left(v_0^2+\bar{c}^2\right)}\delta(y)\right]. \tag{29}$$

Imposing the normalization condition $\int_{-\infty}^{+\infty} dy P(y) = 1$ then allows us to determine a as

$$a = \frac{1}{2}\,\frac{\bar{c}\gamma}{v_0^2 - \bar{c}^2}, \tag{30}$$

which leads to the final explicit result for the stationary probability $P_{\sigma_1,\sigma_2}(y)$,

$$P_{\sigma_1,\sigma_2}(y) = \frac{\gamma\bar{c}}{4\left(v_0^2+\bar{c}^2\right)}\; e^{-\frac{2\gamma\bar{c}}{v_0^2-\bar{c}^2}|y|}\begin{pmatrix} 1 \\ \frac{v_0+\bar{c}}{v_0-\bar{c}}\theta(y) + \frac{v_0-\bar{c}}{v_0+\bar{c}}\theta(-y) \\ \frac{v_0-\bar{c}}{v_0+\bar{c}}\theta(y) + \frac{v_0+\bar{c}}{v_0-\bar{c}}\theta(-y) \\ 1 \end{pmatrix}$$
$$+ \frac{1}{2}\,\frac{\bar{c}^2}{v_0^2+\bar{c}^2}\delta(y)\begin{pmatrix}1\\0\\0\\1\end{pmatrix}, \tag{31}$$

as well as the total probability,

$$P(y) = \frac{\bar{c}\gamma v_0^2}{v_0^4 - \bar{c}^4}\; e^{-\frac{2\gamma\bar{c}}{v_0^2-\bar{c}^2}|y|} + \frac{\bar{c}^2}{v_0^2+\bar{c}^2}\delta(y). \tag{32}$$

In Fig. 2 we compare our theoretical results for $P_{\sigma_1,\sigma_2}(y)$ in Eq. (31) for $v_0 = 1$, $\bar{c} = 1/2$, $\gamma = 1/2$ and $D = 0$ with numerical simulations, showing a perfect agreement [note that, to keep the figure readable, the Dirac δ components of $P_{++}(y)$ and $P_{--}(y)$ are not shown there although they are clearly seen on the simulations—see also Fig. 1—and we have checked that their associated weight fully agrees with the prediction in Eq. (31)]. In Fig. 3 we compare our result for the total probability $P(y)$ in Eq. (32) for two different values of $c = 0.5$ and $c = 0.8$ (and $v_0 = 1$, $\gamma = 1/2$, and $D = 0$) with numerical simulations, showing also a very good agreement.

Note also that for each state (σ_1, σ_2) one can check from Eq. (31) that $\int_{-\infty}^{+\infty} dy P_{\sigma_1,\sigma_2}(y) = \frac{1}{4}$, hence each of the four states is equiprobable in the stationary solution, as expected. The variance of the position is

$$\int_{-\infty}^{+\infty} dy\, y^2\, P(y) = \frac{v_0^2}{2\gamma^2\bar{c}^2}\,\frac{\left(v_0^2-\bar{c}^2\right)^2}{v_0^2+\bar{c}^2}. \tag{33}$$

In the passive limit $\gamma, v_0 \to +\infty$ with $D_{\rm eff} = v_0^2/(2\gamma)$, as well as $\bar{c}$, fixed, the weight of the δ function vanishes as $\bar{c}^2/v_0^2$

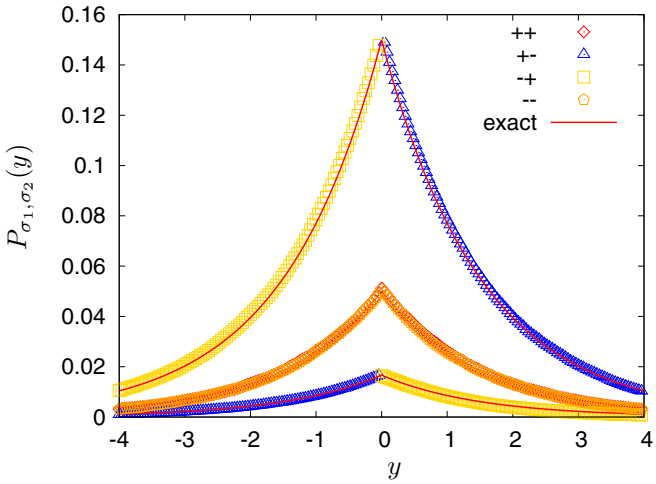

FIG. 2. Plot of $P_{\sigma_1,\sigma_2}(y)$ vs y for $v_0 = 1$, $\bar{c} = 1/2$, $\gamma = 1/2$ and $D = 0$. The symbols correspond to numerical simulations for $\sigma_1 = \pm1$, $\sigma_2 = \pm1$, obtained by solving Eq. (10), while the solid line corresponds to the exact result in Eq. (31). Note that $P_{++}(y) = P_{--}(y)$ and $P_{+-}(y) = P_{-+}(-y)$ as consequences of the unicity of the stationary state and of the symmetries discussed below in Eq. (72). Note that $P_{+-}(y)$ as well as $P_{-+}(y)$ are both discontinuous at $y = 0$, in agreement with Eq. (31). Instead, $P_{++}(y) = P_{--}(y)$ exhibit a Dirac δ component $\propto \delta(y)$ which, for clarity, is not shown on the figure, although it is clearly seen on the simulation and its weight is in full agreement with the prediction in Eq. (31).

and one recovers the standard Gibbs-Boltzmann distribution

$$P(y) \to \frac{\bar{c}}{2D_{\rm eff}}e^{-\bar{c}|y|/D_{\rm eff}}, \quad P_{\sigma_1,\sigma_2}(y) \to \frac{1}{4}\,\frac{\bar{c}}{2D_{\rm eff}}e^{-\bar{c}|y|/D_{\rm eff}}, \tag{34}$$

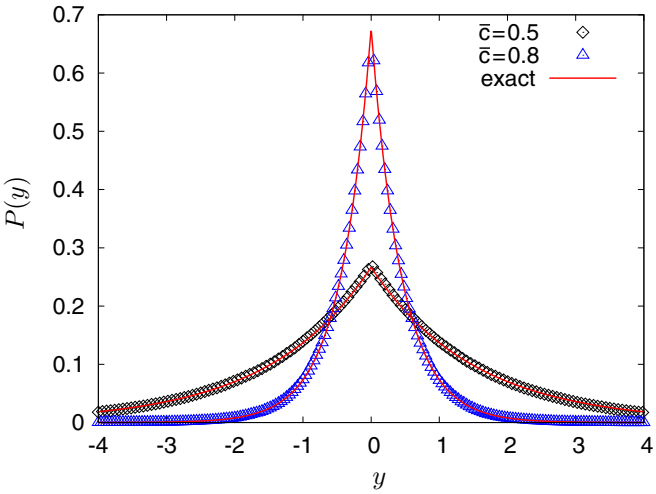

FIG. 3. Plot of the total probability density $P(y)$ vs y for two different values of the interaction strength $\bar{c} = 0.5$ and $\bar{c} = 0.8$ for $v_0 = 1$, $\gamma = 1/2$ and $D = 0$. The symbols are the results of numerical simulations, obtained by solving Eq. (10), while the solid lines correspond to the exact result in Eq. (32). Note that, for clarity, the Dirac δ component $\propto \delta(y)$ is not shown here although it is clearly seen in the simulations and its weight is in full agreement with the prediction in Eq. (32).

for all σ_1, σ_2. Therefore, the δ peak in Eq. (32) in the stationary distribution is an explicit signature of the activity in the system. Note that even for finite v_0, the non-δ function part of $P(y)$ in Eq. (32) retains a pure symmetric-exponential form $\propto e^{-\mu|y|}$, as in the passive case, albeit with a different decay rate $\mu = 2\gamma\bar{c}/(v_0^2 - \bar{c}^2)$ from the passive case $\propto e^{-\bar{c}|y|/D_{\rm eff}}$.

When $v_0 \to \bar{c}^+$ each term in $P(y)$ in Eq. (32) goes to $\frac{1}{2}\delta(y)$ and the size of the bound state goes to zero. To investigate the fine structure inside the critical regime, one can rescale y by the typical size of the bound state. Denoting $y = \frac{v_0 - \bar{c}}{\gamma}\tilde{y}$ one obtains the scaling form in the critical region as

$$P(y)dy = \tilde{P}(\tilde{y})d\tilde{y}, \quad \tilde{P}(\tilde{y}) = \frac{1}{4}e^{-|\tilde{y}|}\begin{pmatrix}0\\1\\1\\0\end{pmatrix} + \frac{1}{2}\delta(\tilde{y})\begin{pmatrix}1\\0\\0\\1\end{pmatrix}. \tag{35}$$

The first part shows that when they have opposite velocities $\sigma_1 = -\sigma_2$ the two RTPs form a (very small) exponential bound state (weak clustering), while when they have identical velocities they are bound at exactly the same position in space (strong clustering).

B. With thermal noise, $D > 0$

We now switch on a nonzero value of D in Eq. (8). As a result, the FP equation for $P_{\sigma_1,\sigma_2}(y,t)$ changes from Eq. (9) to

$$\partial_t P_{\sigma_1,\sigma_2} = -\partial_y\{[-2\bar{c}\,\mathrm{sgn}(y) + v_0(\sigma_1 - \sigma_2)]P_{\sigma_1,\sigma_2}\} - 2\gamma P_{\sigma_1,\sigma_2} + \gamma\left(P_{-\sigma_1,\sigma_2} + P_{\sigma_1,-\sigma_2}\right) + 2D\partial_y^2 P_{\sigma_1,\sigma_2}, \tag{36}$$

where only the last term on the r.h.s., involving the second derivative with respect to y, is D-dependent. We now look for a stationary solution, setting $\partial_t P_{\sigma_1,\sigma_2} = 0$ on the l.h.s of Eq. (36). Since $D > 0$ this solution will obey:

(i) continuity of $P_{\sigma_1,\sigma_2}(y)$ at $y = 0$,

(ii) a jump in the derivative at zero, with the matching condition

$$P'_{\sigma_1,\sigma_2}(0^+) - P'_{\sigma_1,\sigma_2}(0^-) = -2\frac{\bar{c}}{D}P_{\sigma_1,\sigma_2}(0). \tag{37}$$

These give two sets of four conditions, since they hold for any σ_1, σ_2. As discussed in Sec. II, we anticipate that the presence of a finite D will smear out the δ function and replace it by a cusp at $y = 0$ and exponential decaying profile, whose width will vanish as $D \to 0^+$. Since, up to the sign of y, Eq. (36) is linear with constant coefficients, it will be a linear superposition of exponentials for $y > 0$ and $y < 0$ separately. We thus look for a particular solution of the form

$$P_{\sigma_1,\sigma_2}(y) = A^{\epsilon}_{\sigma_1,\sigma_2}e^{-\mu|y|}, \tag{38}$$

where $\epsilon = \mathrm{sgn}(y)$.

Let us start by determining μ. Inserting Eq. (38) in Eq. (36) in the stationary state we find that the amplitude vector A^{ϵ} must satisfy the same condition Eq. (18) where now the matrix $\mathcal{M}_{\pm}(\mu)$ has an additional D-dependent diagonal term

$$\mathcal{M}_{\epsilon}(\mu) = (-2\mu\bar{c} + 2D\mu^2 - 2\gamma)\,\mathbb{I} + M(\epsilon\mu), \tag{39}$$

with $M(\mu)$ given in Eq. (19). The eigenvalues of $\mathcal{M}_{\epsilon}(\mu)$ and their associated eigenvectors are then

$$-2\mu\bar{c} + 2D\mu^2 - 2\gamma, \quad V^1, \tag{40}$$

$$-2\mu\bar{c} + 2D\mu^2 - 2\gamma, \quad V^2(\epsilon\mu), \tag{41}$$

$$-2\mu\bar{c} + 2D\mu^2 - 2\gamma - 2\sqrt{\gamma^2 + \mu^2 v_0^2}, \quad V^3(\epsilon\mu), \tag{42}$$

$$-2\mu\bar{c} + 2D\mu^2 - 2\gamma + 2\sqrt{\gamma^2 + \mu^2 v_0^2}, \quad V^4(\epsilon\mu), \tag{43}$$

where the eigenvectors $\hat{O} = [V^1, V^2(\mu), V^3(\mu), V^4(\mu)]$ are given (in column form) in Eq. (21) and depend on μ via $\bar{c}$ and s. As in the previous subsection, the value of μ is fixed by the condition

$$\begin{aligned}\det \mathcal{M}_{\epsilon}(\mu) &= (-2\mu\bar{c} + 2D\mu^2 - 2\gamma)^2 \\ &\times \left(-2\mu\bar{c} + 2D\mu^2 - 2\gamma - 2\sqrt{\gamma^2 + \mu^2 v_0^2}\right) \\ &\times \left(-2\mu\bar{c} + 2D\mu^2 - 2\gamma + 2\sqrt{\gamma^2 + \mu^2 v_0^2}\right) \\ &= 0.\end{aligned} \tag{44}$$

1. First two eigenvectors

Setting the first factor in Eq. (44) to 0 (corresponding to the sectors of the two first eigenvectors V^1 and V^2) we get

$$-2\mu\bar{c} + 2D\mu^2 - 2\gamma = 0. \tag{45}$$

Taking the positive root we obtain

$$\mu = \mu_1 = \mu_2 = \frac{\bar{c} + \sqrt{\bar{c}^2 + 4D\gamma}}{2D}, \tag{46}$$

which corresponds to a component of $P_{\sigma_1,\sigma_2}(y)$ proportional to $e^{-\frac{\bar{c}+\sqrt{\bar{c}^2+4D\gamma}}{2D}|y|}$. In the limit $D \to 0$ this component yields the $\delta(y)$ term obtained in the previous section for $D = 0$ [see Eq. (31)].

2. The two other eigenvectors

The third and the fourth factors in Eq. (44) (corresponding to the eigenvectors V^3 and V^4) lead to the pair of equations

$$-\mu\bar{c} + D\mu^2 - \gamma + \nu\sqrt{\gamma^2 + \mu^2 v_0^2} = 0, \tag{47}$$

with $\nu = -1$ for V^3 and $\nu = +1$ for V^4. For $D = 0$ one finds the solutions $\mu = 0$ and $\mu = \frac{2\bar{c}\gamma}{v_0^2 - \gamma^2}$ found previously. For $D > 0$, let us use dimensionless units. We write $\mu = \frac{\gamma}{v_0}\tilde{\mu}$ and look for the positive roots $\tilde{\mu}$ of

$$f_{\eta}(\tilde{\mu}) = -g\tilde{\mu} + \tilde{D}\tilde{\mu}^2 - 1 + \nu\sqrt{1 + \tilde{\mu}^2} = 0, \tag{48}$$

in terms of the two dimensionless parameters

$$g = \frac{\bar{c}}{v_0}, \quad \tilde{D} = \frac{D\gamma}{v_0^2}. \tag{49}$$

Taking the square of Eq. (48) one finds a quartic equation for $\tilde{\mu}$. However, one can easily check that there is a trivial solution $\tilde{\mu} = 0$, which is of course discarded since we need $\tilde{\mu} > 0$. This leads to a cubic equation for $\tilde{\mu}$,

$$-2g + \tilde{\mu}(2\tilde{D} + 1 - g^2) + 2g\tilde{D}\tilde{\mu}^2 - \tilde{D}^2\tilde{\mu}^3 = 0. \tag{50}$$

Note that after squaring Eq. (48) the ν-dependence has disappeared. Thus, the information about the associated eigenvenctor (V^3 or V^4) has been lost. Hence, we need to reinject the solution for $\tilde{\mu}$ [from Eq. (50)] back into the original unsquared Eq. (48) to recover the eigenvector dependence. Indeed, by noting that $\sqrt{1+\tilde{\mu}^2} > 0$ and $\nu = \pm 1$, it follows from Eq. (48) that

$$\nu = \mathrm{sgn}(1 + g\tilde{\mu} + \tilde{D}\tilde{\mu}^2), \tag{51}$$

with $\nu = -1$ associated to V^3 while $\nu = +1$ associated to V^4.

To solve the cubic Eq. (50) we first rewrite it in the standard form, by writing $\tilde{\mu} = t + 2g/(3\tilde{D})$, which gives $t^3 + pt + q = 0$ with

$$p = -\frac{6\tilde{D} + g^2 + 3}{3\tilde{D}^2}, \quad q = \frac{2g(9\tilde{D} + g^2 - 9)}{27\tilde{D}^3}, \tag{52}$$

and the discriminant is given by

$$\Delta_2 = -(4p^3 + 27q^2) = 4\tilde{D}^{-6}[(\tilde{D}^2 + 10\tilde{D} - 2)g^2 + (2\tilde{D}+1)^3 + g^4]. \tag{53}$$

It is easy to see that Δ_2 is always positive, hence there are three real roots indexed by $k = 0, 1, 2$ and given by the Cardano formula [31]

$$t_k = 2\sqrt{-\frac{p}{3}}\cos\left[\frac{1}{3}\arccos\left(\frac{3q}{2p}\sqrt{-\frac{3}{p}}\right) - \frac{2\pi k}{3}\right], \quad k = 0, 1, 2. \tag{54}$$

This leads to three possible roots in the original variable $\tilde{\mu}$

$$\tilde{\mu}_k = \frac{2g}{3\tilde{D}} + \frac{2}{3}\sqrt{\frac{6\tilde{D} + g^2 + 3}{\tilde{D}^2}} \times \cos\left\{\frac{1}{3}\cos^{-1}\left[-\frac{g(9\tilde{D} + g^2 - 9)}{(6\tilde{D} + g^2 + 3)^{3/2}}\right] - \frac{2\pi k}{3}\right\}. \tag{55}$$

By investigating Eq. (55) using Mathematica, we find that

$$\tilde{\mu}_0 > \tilde{\mu}_1 > 0, \quad \tilde{\mu}_2 < 0. \tag{56}$$

Since $\tilde{\mu}_2 < 0$ we discard this root. Thus, the only allowed roots are $\tilde{\mu}_0$ and $\tilde{\mu}_1$. Now using Eq. (51), we find that the values of ν associated to these two roots are, respectively, $\nu = -1$ for $\tilde{\mu}_0$ and $\nu = +1$ for $\tilde{\mu}_1$. Thus, $\tilde{\mu}_0$ is associated to the eigenvector V^3 while $\tilde{\mu}_1$ is associated to V^4. Hence, in summary the only positive roots are

$$\mu_3 = \frac{\gamma}{v_0}\tilde{\mu}_0, \quad V^3, \qquad \mu_4 = \frac{\gamma}{v_0}\tilde{\mu}_1, \quad V^4. \tag{57}$$

To conclude, the general solution is

$$P_{\sigma_1,\sigma_2}(y) = \{[b_1 V^1_{\sigma_1,\sigma_2} + b_2 V^2_{\sigma_1,\sigma_2}(\mu_2)]\theta(y) + [b_1' V^1_{\sigma_1,\sigma_2} + b_2' V^2_{\sigma_1,\sigma_2}(-\mu_2)] \times \theta(-y)\}e^{-\mu_2|y|} + [b_3 V^3_{\sigma_1,\sigma_2}(\mu_3)\theta(y) + b_3' V^3_{\sigma_1,\sigma_2}(-\mu_3)\theta(-y)]e^{-\mu_3|y|} + [b_4 V^4_{\sigma_1,\sigma_2}(\mu_4)\theta(y) + b_4' V^4_{\sigma_1,\sigma_2} \times (-\mu_4)\theta(-y)]e^{-\mu_4|y|}. \tag{58}$$

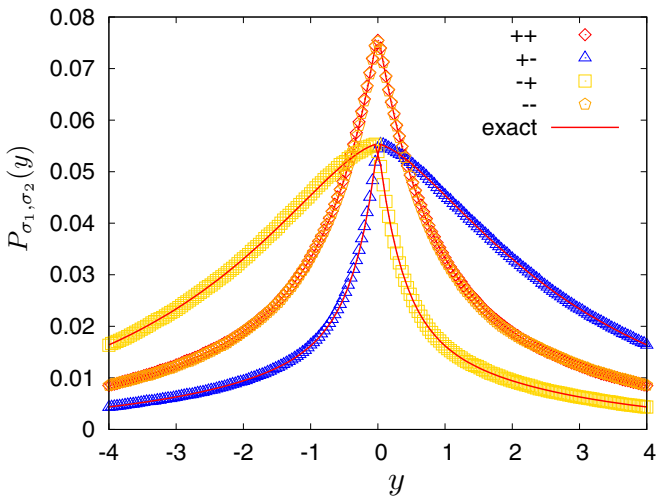

FIG. 4. Plot of $P_{\sigma_1,\sigma_2}(y)$ vs y for $v_0 = 1$, $\bar{c} = 1/2$, $\gamma = 1/2$ and $D = 1/2$. The symbols correspond to numerical simulations for $\sigma_1 = \pm 1$, $\sigma_2 = \pm 1$ while the solid line corresponds to the exact result in Eq. (A16). Note that $P_{++}(y) = P_{--}(y)$ $P_{+-}(y) = P_{-+}(-y)$ as a consequences of the unicity of the stationary state and of the symmetries discussed below in Eq. (72).

To determine the eight coefficients b_i, b_i' we can use (i) the continuity of $P_{\sigma_1,\sigma_2}(y)$ at $y = 0$ (four equations), (ii) the four matching conditions Eq. (37),

$$P'_{\sigma_1,\sigma_2}(0^+) - P'_{\sigma_1,\sigma_2}(0^-) = -2\frac{\bar{c}}{D}P_{\sigma_1,\sigma_2}(0), \tag{59}$$

and then the normalization condition for the total probability $P(y) = \sum_{\sigma_1=\pm1}\sum_{\sigma_2=\pm1} P_{\sigma_1,\sigma_2}(y)$, i.e., $\int_{-\infty}^{+\infty} dy P(y) = 1$. This is performed in the Appendix, leading to the result given in Eq. (A16). In Fig. 4, we compare this analytical predictions for $P_{\sigma_1,\sigma_2}(y)$ in Eq. (A16) for a specific set of the parameters of the model to numerical simulations, showing an excellent agreement.

To conclude this section, we provide our explicit results for the final result for the total probability $P(y)$,

$$P(y) = \frac{1}{2\left(\frac{c_2}{\mu_2} + \tilde{b}_3\frac{s_3-1}{\mu_3} + \tilde{b}_4\frac{s_4+1}{\mu_4}\right)}[c_2 e^{-\mu_2|y|} + \tilde{b}_3(s_3-1)e^{-\mu_3|y|} + \tilde{b}_4(s_4+1)e^{-\mu_4|y|}], \tag{60}$$

$$\tilde{b}_3 = \frac{s_2(\bar{c} - D\mu_4)}{(c_3+c_4)\bar{c} - D(c_4\mu_3 + c_3\mu_4)}, \qquad \tilde{b}_4 = \frac{s_2(\bar{c} - D\mu_3)}{(c_3+c_4)\bar{c} - D(c_4\mu_3 + c_3\mu_4)}, \tag{61}$$

and we recall that

$$c_i = -\frac{\mu_i v_0}{\sqrt{\gamma^2 + \mu_i^2 v_0^2}}, \quad s_i = \frac{\gamma}{\sqrt{\gamma^2 + \mu_i^2 v_0^2}}, \tag{62}$$

where μ_2 is given in Eq. (46), and μ_3 and μ_4 are given in Eqs. (55)–(57). For instance, for $\bar{c} = 1/2$, $D = 1/2$, $v_0 = 1$, and $\gamma = 1/2$ we find

$$P(y) = 0.020441\, e^{-3.3234y} + 0.0868356\, e^{-1.61803y} + 0.157553\, e^{-0.357926y}, \tag{63}$$

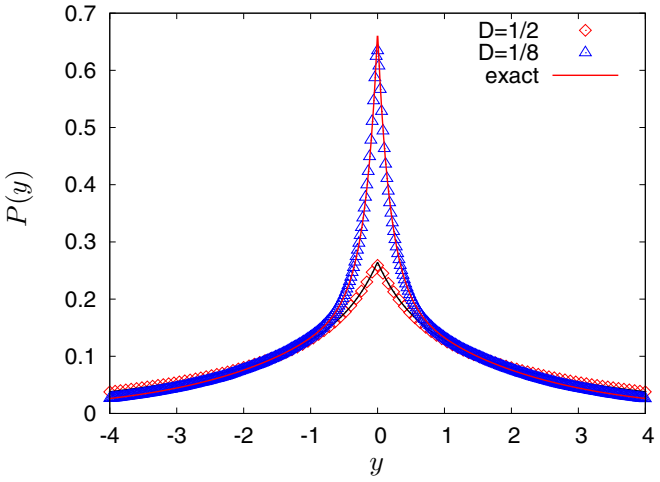

FIG. 5. Plot of the total probability density $P(y)$ vs y for two different values the diffusion constant $D = 1/2$ and $D = 1/8$ and for $\bar{c} = 0.5$, $v_0 = 1$, $\gamma = 1/2$. The symbols are the results of numerical simulations while the solid lines correspond to the exact results in Eq. (63) for $D = 1/2$ and in Eq. (64) for $D = 1/8$.

while for $\bar{c} = 1/2$, $D = 1/8$, $v_0 = 1$, and $\gamma = 1/2$ we find

$$P(y) = 0.0523053\, e^{-12.331y} + 0.397104\, e^{-4.82843y} + 0.220603\, e^{-0.533482y}. \quad (64)$$

These theoretical predictions in Eqs. (63) and (64) are compared to numerical simulations in Fig. 5, showing a very good agreement.

IV. MORE GENERAL INTERACTION WITHOUT DIFFUSION

A. Models and flow diagram

In this section we discuss the case of a more general attractive interaction between the two RTPs, i.e., a more general force $f(y)$ which is an odd function of y, $f(-y) = -f(y)$. For simplicity, we will set $D = 0$ as argued earlier. In this case, the equations for the center of mass $w = (x_1 + x_2)/2$ and the relative coordinate $y = x_1 - x_2$, respectively, in Eqs. (5) and (6) reduce to

$$\frac{dw}{dt} = \frac{v_0}{2}\,[\sigma_1(t) + \sigma_2(t)], \quad (65)$$

$$\frac{dy}{dt} = 2f(y) + v_0\,[\sigma_1(t) - \sigma_2(t)]. \quad (66)$$

In principle, we can write down the FP equation for the joint distribution $P_{\sigma_1,\sigma_2}(w, y, t)$. This joint distribution obviously does not reach a steady state, since $w(t)$ in Eq. (65) corresponds to a free RTP motion and hence diffuses at late times. Only the marginal distribution of the relative coordinate $P_{\sigma_1,\sigma_2}(y, t) = \int_{-\infty}^{+\infty} dw\, P_{\sigma_1,\sigma_2}(w, y, t)$ reaches a steady state as $t \to \infty$. Hence, we focus on the y-marginal only. The FP equation for $P_{\sigma_1,\sigma_2}(y, t)$ reads

$$\partial_t P_{\sigma_1,\sigma_2} = -\partial_y\big\{[2f(y) + v_0(\sigma_1 - \sigma_2)]P_{\sigma_1,\sigma_2}\big\} - 2\gamma P_{\sigma_1,\sigma_2} + \gamma\big(P_{-\sigma_1,\sigma_2} + P_{\sigma_1,-\sigma_2}\big). \quad (67)$$

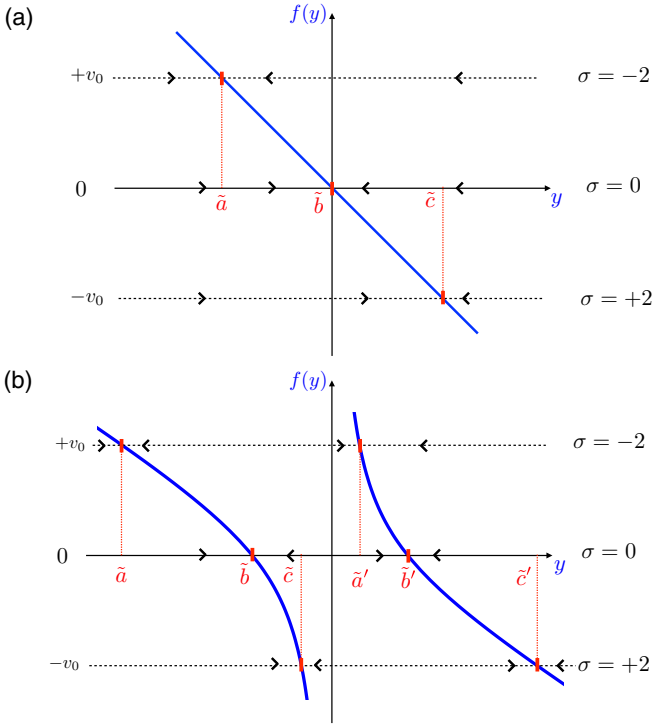

FIG. 6. Dynamical diagrams for the 2 RTPs within the two models discussed in the text. The interaction force between the RTPs, $f(y)$ is plotted versus y, the relative coordinate. The fixed points for the dynamics (66) in each state of the two RTPs are determined by the roots of the equations $f(y) = -v_0$ (state $+-$), $f(y) = 0$ (states $++$ and $--$) and $f(y) = v_0$ (state $-+$). These are obtained as the intersections of the plot of $f(y)$ with the three horizontal lines which correspond to the three possible values of $\sigma = \sigma_1 - \sigma_2$. (a) The harmonic force model, $f(y) = -y$, with the three fixed points $\tilde{a}$, $\tilde{b}$ and $\tilde{c}$ (see discussion in the text). The flow indicated by the arrows shows the dynamics of $y(t)$ in each state. The three fixed points are attractive and the steady state is supported by the interval $[a, c]$. (b) The second model (with a repulsive short range interaction), $f(y) = \frac{1}{y} - y$, with the six fixed points $\tilde{a}, \tilde{b}, \tilde{c}$ and $\tilde{a}', \tilde{b}', \tilde{c}'$ (see discussion in the text). All fixed points are attractive. The steady state is not unique, with two supports $[\tilde{a}', \tilde{c}']$ and $[\tilde{a}, \tilde{c}]$, depending on the initial ordering of the particles.

Note that for $f(y) = -\bar{c}\,\mathrm{sgn}(y)$ discussed in Sec. III, this equation reduces to Eq. (9).

To search for a stationary solution $P_{\sigma_1,\sigma_2}(y)$, one must set the l.h.s. of Eq. (67) to 0. However, before writing the steady-state equations, it is useful to see what we can anticipate about the form of this solution, and in particular whether this solution is unique. This can be investigated by studying the stability behavior of the Langevin Eq. (66), following the examples in Refs. [16,20]. We will consider two generic examples of interactions between the RTPs, which present a different steady-state behavior. The first example is the harmonic force $f(y) = -\lambda y$. In the second example there is in addition a repulsion between the particles so that they cannot cross, with $f(y) = \frac{1}{y} - \lambda y$. The curves $f(y)$ versus y are plotted in Fig. 6 for both examples. Note that $\sigma_1(t) - \sigma_2(t)$ can take only three values $(-2, 0, 2)$ corresponding, respectively, to the two RTPs being in the states $(-+)$, $(++)$ or

$(--)$ and $(+-)$. Hence, to find stationary points for a fixed two-particle state one must look at the roots of the equations, respectively, $f(y) = v_0$, $f(y) = 0$ and $f(y) = -v_0$. In Fig. 6 we have indicated the positions of these roots. In the first example (harmonic force) there are three of them denoted $\tilde{a}$, $\tilde{b}$, and $\tilde{c}$. Because of the symmetry $f(-y) = -f(y)$ one has $\tilde{b} = 0$ and $\tilde{c} = -\tilde{a} = \lambda/v_0$. In the second example (with short range repulsion) there are six of them: three on the $y < 0$ side (i.e., $x_1 < x_2$) denoted $\tilde{a}$, $\tilde{b}$, and $\tilde{c}$ and three on the $y > 0$ positive side (i.e., $x_1 > x_2$), denoted $\tilde{a}'$, $\tilde{b}'$, and $\tilde{c}'$. Because of the symmetry $f(-y) = -f(y)$ one has $\tilde{a}' = -\tilde{c}$, $\tilde{b}' = -\tilde{b}$, and $\tilde{c}' = -\tilde{a}$. We have indicated by arrows in the figure the flow diagram for each of the three values of $\sigma = \sigma_1(t) - \sigma_2(t)$. For both examples considered here all fixed points $\tilde{a}, \tilde{b}, \tilde{c}$ (and $\tilde{a}', \tilde{b}', \tilde{c}'$) are attractive [i.e., $f'(y)$ is negative at the fixed point]. From the general analysis performed in Ref. [20], we can predict the support of the steady-state probabilities from the flow in the Fig. 6.

In the first model (harmonic force) we predict that the stationary state is unique and that after a finite time the relative coordinate $y(t)$ will end up within the interval $[\tilde{a}, \tilde{c}]$. Once the particle enters this interval $[\tilde{a}, \tilde{c}]$, it can never go out via the dynamics in Eq. (66). Hence, we would expect that the stationary state, if it exists, will be supported only inside the interval $[\tilde{a}, \tilde{c}]$. In other words, the stationary probability density $P_{\sigma_1,\sigma_2}(y)$ will strictly vanish outside this interval $[\tilde{a}, \tilde{c}]$.

In the second model (with short range repulsion) the two RTPs cannot cross, hence it is clear that, depending on the initial condition, i.e., whether $x_1(0) > x_2(0)$ or $x_2(0) > x_1(0)$, the relative coordinate $y(t)$ of the two RTPs will end up either on $[\tilde{a}, \tilde{c}]$ or on $[\tilde{a}', \tilde{c}']$. In that case the stationary solution is not unique, and there are two possible disconnected supports, which are images of each other by the symmetry $y \to -y$.

B. Determination of the steady-state solution

We now focus on the case where the stationary solution is unique (for models in the same class as the harmonic well where the potential has a single minimum) and show how to find this solution. Let us rewrite the equation Eq. (67) in components and set $\partial_t P_{\sigma_1,\sigma_2}(y,t) = 0$, leading to the four coupled equations

$$\partial_t P_{++} = -2\partial_y(f(y)P_{++}) - 2\gamma P_{++} + \gamma(P_{+-} + P_{-+}) = 0, \tag{68}$$

$$\partial_t P_{+-} = -2v_0\partial_y P_{+-} - 2\partial_y(f(y)P_{+-}) - 2\gamma P_{+-} + \gamma(P_{++} + P_{--}) = 0, \tag{69}$$

$$\partial_t P_{-+} = 2v_0\partial_y P_{-+} - 2\partial_y(f(y)P_{-+}) - 2\gamma P_{-+} + \gamma(P_{++} + P_{--}) = 0, \tag{70}$$

$$\partial_t P_{--} = -2\partial_y(f(y)P_{--}) - 2\gamma P_{--} + \gamma(P_{+-} + P_{-+}) = 0. \tag{71}$$

These equations [see also Eq. (67)] are invariant under the change $(y, \sigma_1, \sigma_2) \to (y, -\sigma_2, -\sigma_1)$. Since $f(y)$ is an odd function of y, they are also invariant under the change $(y, \sigma_1, \sigma_2) \to (-y, -\sigma_1, -\sigma_2)$. Since we consider here the case where the stationary solution is unique, this implies that

$$P_{\sigma_1,\sigma_2}(y) = P_{-\sigma_1,-\sigma_2}(-y), \quad P_{\sigma_1,\sigma_2}(y) = P_{\sigma_2,\sigma_1}(-y), \tag{72}$$

where the second symmetry is obtained by combining the two symmetries mentioned above. The first corresponds to reversing the speed of each particle and reversing the direction of y. Since the confining potential $V(y)$ is symmetric under $y \to -y$ [equivalently $f(-y) = -f(y)$], the first symmetry in Eq. (72) is evident when the stationary state is unique. Summing over σ_1, σ_2 this also implies that the total probability $P(y)$ must be an even function of y.

It is convenient to introduce the following quantities:

$$p_1 = P_{++} + P_{--}, \quad p_2 = P_{++} - P_{--},$$
$$q_1 = P_{+-} + P_{-+}, \quad q_2 = P_{+-} - P_{-+}, \quad P = p_1 + q_1. \tag{73}$$

In terms of these quantities Eqs. (68)–(71) simplify to

$$-\partial_y[f(y)p_1] - \gamma p_1 + \gamma q_1 = 0, \tag{74}$$

$$-\partial_y[f(y)p_2] - \gamma p_2 = 0, \tag{75}$$

$$-\partial_y[f(y)q_1 + v_0 q_2] - \gamma q_1 + \gamma p_1 = 0, \tag{76}$$

$$-\partial_y[f(y)q_2 + v_0 q_1] - \gamma q_2 = 0. \tag{77}$$

Amazingly, Eq. (75) for $p_2(y)$ completely decouples from p_1, q_1 and q_2 for arbitrary $f(y)$. In fact p_2 is not needed to obtain p_1, q_1, and q_2. The origin of this simplification will be discussed below. It therefore remains to solve the three Eqs. (74), (76), and (77). Adding Eqs. (74) and (76) and using $P = p_1 + q_1$ one finds

$$\partial_y(2f(y)P(y) + 2v_0 q_2(y)) = 0 \implies 2f(y)P(y) + 2v_0 q_2(y) = J, \tag{78}$$

where J is a constant. We can identify this constant with the total probability current in the system. This can be seen by adding the four Eqs. (67) for $\sigma_1 = \pm 1$ and $\sigma_2 = \pm 1$ which gives $\partial_t P = -\partial_y J(y)$ with $J(y) = 2f(y)P(y) + 2v_0 q_2(y)$. In the steady state, the probability current must be a constant since $\partial_t P = 0$. Hence, $J(y) = J$ is independent of y and coincides with Eq. (78). Since $f(y)$ is an odd function, $P(y)$ is even, and $q_2(y)$ is also an odd function because of the symmetry Eq. (72) and of the unicity of the steady state, Eq. (78) implies that the current J must vanish. Setting $J = 0$ we get another relation,

$$f(y)P(y) = f(y)(p_1(y) + q_1(y)) = -v_0 q_2(y). \tag{79}$$

We now eliminate $q_2(y)$ from Eqs. (76) and (77) by using the relation in Eq. (79). This gives a pair of coupled equations, involving $P(y)$ and $q_1(y)$,

$$-\partial_y(f(y)(q_1 - P)) + \gamma P - 2\gamma q_1 = 0, \tag{80}$$

$$-\partial_y\left(v_0^2 q_1 - f(y)^2 P\right) + \gamma f(y) P = 0, \tag{81}$$

which can be conveniently rewritten as

$$fP' + (f' + \gamma)P = fq_1' + (f' + 2\gamma)q_1, \tag{82}$$

$$f^2 P' + f(2f' + \gamma)P = v_0^2 q_1'. \tag{83}$$

After differentiating both Eqs. (82) and (83) and performing straightforward manipulations, one can eliminate q_1 and write a closed second-order ordinary differential equation for $P(y)$. We get

$$f(y)\left[v_0^2 - f(y)^2\right]P''(y) + \left\{\left[v_0^2 - 3f(y)^2\right][\gamma + 2f'(y)] + \frac{f(y)[f(y)-v_0][f(y)+v_0]f''(y)}{2\gamma + f'(y)}\right\}P'(y) \tag{84}$$

$$+\left\{\frac{\gamma\left[v_0^2 - 3f(y)^2\right]f''(y)}{2\gamma + f'(y)} - f(y)[\gamma + 2f'(y)][2\gamma + 3f'(y)]\right\}P(y) = 0. \tag{85}$$

One can in principle solve this equation for $P(y)$ using the boundary conditions given below. Once $P(y)$ is known one obtains $q_2(y) = -f(y)P(y)/v_0$ from Eq. (79). One also obtains $q_1(y)$ by integration of Eq. (83). Alternatively, a similar second-order differential equation can also be derived for $q_1(y)$ by eliminating $P(y)$ from the pair of Eqs. (82) and (83). We do not write it explicitly here. As argued before, the stationary solution is expected to be supported over the finite interval $[\tilde{a}, \tilde{c}]$ where $f(\tilde{a}) = v_0$ and $f(\tilde{c}) = -v_0$. Therefore, Eq. (84) for $P(y)$ holds for $y \in [\tilde{a}, \tilde{c}]$. In addition, we need to provide the appropriate boundary conditions to find the unique solution. These boundary conditions are nontrivial and we derive them below.

1. Boundary conditions

The main idea is to derive, directly from the Langevin Eq. (66) how the four probabilities $P_{\sigma_1,\sigma_2}(y,t)$ evolve in a small time Δt exactly at the two edges of the support $y = \tilde{a}$ and $y = \tilde{c}$. Let us illustrate this explicitly with the state $P_{++}(y,t)$. For this case, the Langevin Eq. (66) says that in a small time Δt the position of the particle evolves by $\Delta y = 2\,f(y)\,\Delta t$. Therefore, the evolution of the probability density $P_{++}(y,t)$ can be written as

$$P_{++}(y, t+\Delta t) = (1 - 2\gamma\,\Delta t)P_{++}(y - 2\,f(y)\,\Delta t, t) + \gamma\,\Delta t[P_{+-}(y,t) + P_{-+}(y,t)]. \tag{86}$$

This is easily explained since in the time interval $[t, t+\Delta t]$ the velocities $(v_0\sigma_1(t), v_0\sigma_2(t))$ do not change sign with probability $1 - 2\gamma\,\Delta t$. Hence, if the particle wants to be at the location y at time $t + \Delta t$, then it must have been at $y - \Delta y = y - 2\,f(y)\,\Delta t$ at time t. This explains the first term in Eq. (86). In contrast, with probability $\gamma\,\Delta t$, it can come from the state $(+-)$ or $(-+)$ just by flipping the negative velocity. This explains the last two terms in Eq. (86). Now we consider this evolution Eq. (86) exactly at the left edge $y = \tilde{a}$ where we recall that $f(\tilde{a}) = v_0$. Hence, the first term on the r.h.s. of Eq. (86) reads $(1 - 2\gamma\,\Delta t)P_{++}(\tilde{a} - 2v_0\Delta t, t)$. Since $2v_0\Delta t > 0$, the argument $\tilde{a} - 2v_0\Delta t < \tilde{a}$. This means that the argument $\tilde{a} - 2v_0\Delta t$ is outside the left edge of the support where, by definition, there is no particle in the stationary state. Hence, the first term is identically zero at $y = \tilde{a}$. As $\Delta t \to 0$, the last two terms in Eq. (86) also vanish. This gives us the boundary condition in the stationary state

$$P_{++}(y = \tilde{a}) = 0. \tag{87}$$

By repeating this argument for each of the states $(\sigma_1 = \pm 1, \sigma_2 = \pm 1)$ at the two boundaries $\tilde{a}$ and $\tilde{c}$, we find the following set of boundary conditions:

$$P_{++}(\tilde{a}) = P_{++}(\tilde{c}) = 0, \tag{88}$$

$$P_{--}(\tilde{a}) = P_{--}(\tilde{c}) = 0, \tag{89}$$

$$P_{+-}(\tilde{a}) = 0, \tag{90}$$

$$P_{-+}(\tilde{c}) = 0. \tag{91}$$

Note that, due to the symmetry condition Eq. (72), these boundary conditions are not all independent. In fact, there are only four independent boundary conditions. Since our original stationary states Eqs. (68)–(71) are four first-order differential equations (albeit coupled), these four boundary conditions are enough to fix the stationary solution uniquely. Note that these boundary conditions Eqs. (88)–(91) mean that no jump is allowed at these points for these probabilities, which must thus vanish continuously.

Let us now return to the function $p_2(y) = P_{++}(y) - P_{--}(y)$. Using both symmetries in Eq. (72) for $\sigma_1 = \sigma_2 = +$ we obtain that

$$p_2(y) = P_{++}(y) - P_{--}(y) = P_{++}(y) - P_{++}(-y) = 0. \tag{92}$$

Hence, all the components $P_{\sigma_1,\sigma_2}(y)$ of the stationary state can be determined.

C. Harmonic interactions and mapping to a three state model

To illustrate the method, let us consider the example of the harmonic interaction $f(y) = -\lambda y$ in which case Eq. (84) becomes

$$(\gamma - 2\lambda)P'(y)\left(v_0^2 - 3\lambda^2y^2\right) - \lambda yP''(y)\left(v_0^2 - \lambda^2y^2\right) + \lambda y(2\gamma - 3\lambda)(\gamma - 2\lambda)P(y) = 0. \tag{93}$$

Let us first study the special case $\gamma = 2\lambda$, which turns out to be a bit simpler. In that case, indeed, the above equations simplify into

$$y\left(v_0^2 - \lambda^2y^2\right)P''(y) = 0 \tag{94}$$

$$-\lambda yP' + \lambda P = -\lambda yq_1' + 3\lambda q_1, \tag{95}$$

$$\lambda^2y^2P' = v_0^2q_1'. \tag{96}$$

The solution is easily obtained for $y \in [-\frac{v_0}{\lambda}, \frac{v_0}{\lambda}]$ as

$$P(y) = \frac{\lambda^2}{v_0^2}\left(\frac{v_0}{\lambda} - |y|\right), \quad q_1(y) = \frac{1}{3}\frac{\lambda}{v_0} - \frac{\lambda^4}{3v_0^4}\mathrm{sgn}(y)y^3,$$

$$q_2(y) = \frac{\lambda^3}{v_0^3}y\left(\frac{v_0}{\lambda} - |y|\right), \tag{97}$$

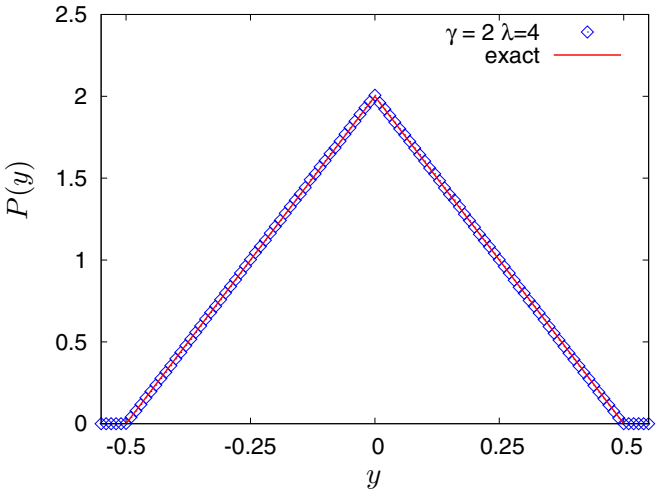

FIG. 7. Plot of the total probability density $P(y)$ vs y for the harmonic interaction $f(y) = -\lambda y$ with $v_0 = 1$, $\lambda = 2$ and $\gamma = 2\lambda = 4$. The symbols are the results of numerical simulations while the solid lines correspond to the exact result in Eq. (97).

and zero for $|y| > \frac{v_0}{\lambda}$. In Fig. 7 we show a comparison of our exact prediction in Eq. (97) with numerical simulations for $\gamma = 2\lambda = 4$ (as well as $v_0 = 1.0$) showing a very good agreement.

The general solution of Eq. (93) can be obtained in terms of hypergeometric functions. In fact, as we show below, the present problem can be mapped onto a recently studied problem of a single RTP with position y, with three internal states, in an harmonic potential $V(y) = \frac{1}{2}\lambda y^2$, which was solved in terms of hypergeometric functions [19]. This leads to the general result for the solution of the 2 RTP problem with harmonic interaction, i.e., of Eq. (93), as

$$P(y) = A_1 \left\{ {}_2F_1\left[1 - \frac{\beta}{2}, \frac{3}{2} - \beta, \frac{3-\beta}{2}; \left(\frac{\lambda y}{v_0}\right)^2\right] + \frac{2}{\sqrt{\pi}} \frac{\Gamma\left(\frac{3-\beta}{2}\right)\Gamma\left(\beta + \frac{1}{2}\right)}{(1-2\beta)\Gamma\left(\frac{\beta+1}{2}\right)} \left(\frac{\lambda y}{v_0}\right)^{\beta-1} \times {}_2F_1\left[\frac{1}{2}, 1 - \frac{\beta}{2}, \frac{\beta+1}{2}; \left(\frac{\lambda x}{v_0}\right)^2\right] \right\}, \quad -\frac{v_0}{\lambda} \leqslant y \leqslant \frac{v_0}{\lambda}, \tag{98}$$

where $\beta = \gamma/\lambda$ and the amplitude A_1 is given in Eq. (33) of Ref. [19].

The model studied in Ref. [19] is defined by the transition rates between the three states denoted $+1$, 0, -1 as shown in Fig. 8(b). One can identify these states with ours as

$$1 \equiv (+-) \Rightarrow P_1 = P_{+-}, \tag{99}$$

$$-1 \equiv (-+) \Rightarrow P_{-1} = P_{-+}, \tag{100}$$

$$0 \equiv (++) \cup (--) \Rightarrow P_0 = P_{++} + P_{--}. \tag{101}$$

This implies that the probabilities denoted as P, Q, and R in Ref. [19] are related to P, q_1, and q_2 studied here via

$$Q = P_1 + P_{-1} \equiv q_1, \tag{102}$$

$$R = P_1 - P_{-1} \equiv q_2, \tag{103}$$

$$P = P_0 + P_1 + P_{-1} \equiv P. \tag{104}$$

Hence, the solution for these functions obtained there also provide the solution for our model.

D. General mapping to a two-dimensional single-RTP model

In fact, this mapping, between (i) the relative coordinate of a pair of interacting particles and (ii) the position of a single particle in a confining potential subjected to a three-state active noise, actually is more general than just the harmonic interaction and can be extended to arbitrary attractive interaction in (i). The general mapping can be formulated as follows. Consider a single particle on a plane with its coordinates $[y(t), z(t)]$ evolving via the pair of equations

$$\frac{dy(t)}{dt} = f[y(t)] + v_0\sigma_y(t), \tag{105}$$

$$\frac{dz(t)}{dt} = g[z(t)] + v_0\sigma_z(t), \tag{106}$$

where the confining force $f(y)$ in the y direction depends only on y and the confining force $g(z)$ in the z direction depends only on z. In Eqs. (105) and (106), $\sigma_{y,z}(t)$ are the y and z components of a director field which has four possible orientations E (East), N (North), W (West), and S (South), as shown in Fig. 8(a). The transition rates between the different directions of the director field are indicated in Fig. 8(a). The state of the system has four labels E, N, W, and S and hence there are four position distribution functions $\mathcal{P}_E(y, z, t)$, $\mathcal{P}_N(y, z, t)$,

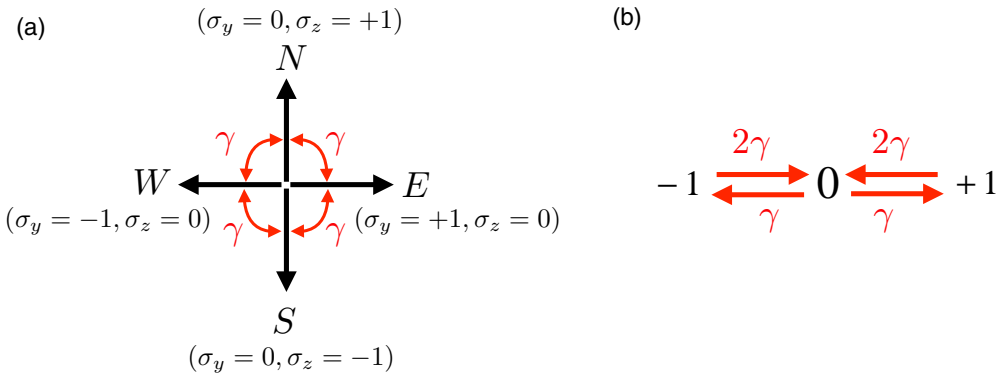

FIG. 8. Illustration of the four-state model (left panel) and corresponding three-state model studied in Ref. [19] and discussed in the text.

$\mathcal{P}_W(y,z,t)$, and $\mathcal{P}_S(y,z,t)$. In Ref. [32], these position distribution functions were computed explicitly in the "free" case where $f(y)=0$ and $g(z)=0$. Here we consider instead the case of nonzero interaction forces $f(y)\neq 0$ and $g(z)\neq 0$. Taking into account the transition rates in Fig. 8(a), one can explicitly write down the associated coupled FP equations [along the lines of Eq. (67)]. We do not repeat them here as they are a bit long [see Eqs. (6a)–(6d) of Ref. [19] in the case $f(y)=-\mu y$ and $g(z)=-\mu z$]. Following Ref. [19] we consider three marginal position distribution in the y direction:

$$P_1(y,t)=\int dz\ \mathcal{P}_E(y,z,t), \tag{107}$$

$$P_{-1}(y,t)=\int dz\ \mathcal{P}_W(y,z,t), \tag{108}$$

$$P_0(y,t)=\int dz\,[\mathcal{P}_N(y,z,t)+\mathcal{P}_S(y,z,t)]. \tag{109}$$

From the explicit FP equations for $\mathcal{P}_{E,N,W,S}$, it is straightforward to obtain the FP equations for these three marginal probability densities proceeding as in Ref. [19]:

$$\frac{\partial}{\partial t}P_1(y,t)=\frac{\partial}{\partial y}[(f(y)-v_0)P_1]+\frac{\gamma}{2}P_0-\gamma P_1, \tag{110}$$

$$\frac{\partial}{\partial t}P_{-1}(y,t)=\frac{\partial}{\partial y}[(f(y)+v_0)P_{-1}]+\frac{\gamma}{2}P_0-\gamma P_{-1}, \tag{111}$$

$$\frac{\partial}{\partial t}P_0(y,t)=\frac{\partial}{\partial y}[f(y)P_0]+\gamma(P_1+P_{-1})-\gamma P_0. \tag{112}$$

We first note that the force field $g(z)$ has completely dropped out in Eqs. (110)–(112) and this is precisely due to the decoupled structure of the force field Eqs. (105) and (106). How is this related to the two-particle model with attractive force $f(y)$? If we take our basic FP equations in Eq. (67) and use the identification in Eqs. (99), (100), and (101), it is easy to see that the resulting FP equations for P_1, P_{-1}, and P_0 are exactly the same as in Eqs. (110)–(112). In fact it is possible by comparing Eqs. (68)–(71) in the present paper, and Eqs. (6a)–(6d) of Ref. [19] to establish a direct mapping between the two interacting RTP model and the single-RTP $2d$-model [19]. One finds

$$\begin{aligned}
P_{+-}(y,t)&=\int dz\ \mathcal{P}_E(y,z,2t),\\
P_{-+}(y,t)&=\int dz\ \mathcal{P}_W(y,z,2t),\\
P_{++}(y,t)&=\int dz\,\mathcal{P}_N(y,z,2t),\\
P_{--}(y,t)&=\int dz\,\mathcal{P}_S(y,z,2t),
\end{aligned} \tag{113, 114}$$

the rescaling of time being equivalent to a rescaling of γ. Note that there is some arbitrariness in connecting $(N,S)\equiv(++,--)$ rather than $(N,S)\equiv(--,++)$. Note that $p_2(y,t)=P_{++}(y,t)-P_{--}(y,t)=\int dz\,[\mathcal{P}_N(y,z,2t)-\mathcal{P}_S(y,z,2t)]$ indeed decouples as found above since it is determined by the dynamics along z (which is not observed). This completes the mapping between the y component of a $2d$ single-particle problem subjected to a force-field as in Eqs. (105) and (106) and the relative coordinate of a pair of RTPs with arbitrary interactions between them.

Finally, it is interesting to observe that if one instead looks at the marginals of the z-coordinate in the $2d$ model (i.e., if we integrate over y instead of z) one has again a mapping to two RTPs interacting with a force $g(z)$, and the identification $W\equiv --$, $E\equiv ++$, $N\equiv +-$, and $S\equiv -+$ [which is obtained by a rotation of the Fig. 8(a)].

V. CONCLUSION

In this paper we have studied two run-and-tumble particles (RTPs) interacting via an attractive potential $V(y)$, depending on their relative coordinate y. In the large time limit, the total probability distribution of y reaches a stationary form $P(y)$ which we have characterized in terms of the solution of a second-order differential equation. For two specific examples of potential $V(y)$ we have obtained the four components of the stationary distribution, $P_{\sigma_1,\sigma_2}(y)$, where $\sigma_1=\pm1$, $\sigma_2=\pm1$ are the states of each RTP with velocity $\pm v_0$.

As a first example, we have studied in detail the case of a linear potential $V(y)\sim|y|$, first without thermal noise (i.e., for $D=0$) and then for general $D>0$. In the first case, $D=0$, a striking result is that $P(y)$ is the sum of a δ function part $\delta(y)$ and a decaying exponential. This is the signature of a strong clustering effect, when the two RTPs are in the same state. This is reminiscent of the observation in [21–24], except that here the clustering effect is enhanced by the attractive interaction. Because of the finite decay length of the exponential part, the weight of the δ part is finite even for an infinite system. In the presence of thermal noise, $D>0$, the δ function broadens and $P(y)$ is now a sum of exponentials. We have tested our analytic formula with numerical simulations of two interacting RTPs.

The second example is the harmonic attraction, $V(y)=\frac{\lambda}{2}y^2$. In that case, the support of $P(y)$ is found to be a finite interval $[-\frac{v_0}{\lambda},\frac{v_0}{\lambda}]$. We found that the general solutions for $P(y)$ on this interval are expressed in terms of hypergeometric functions. In addition, $P_{\sigma_1,\sigma_2}(y)$ generically exhibit power-law singular behaviors at the three points $y=0,\pm\frac{v_0}{\lambda}$. Remarkably, this exact solution can be mapped onto a problem studied previously of a three-state single RTP in one dimension in a harmonic external potential. In fact, as we have shown, this mapping extends to any interaction potential $V(y)$. In addition, a related mapping to a two-dimensional single-RTP model is obtained. Finally, we have also discussed the effect of an additional short-range repulsion. When it is strong enough so that the particles cannot cross it results in the existence of several distinct steady states which are related by the symmetry $y\to -y$.

As we have seen here, it is already nontrivial to obtain the stationary probability for two RTPs with a general interaction potential. An interesting question is whether there are solvable models for a number $N>2$ RTPs. Preliminary study shows that it is already quite challenging for the linear attraction potential. Multiparticle models with $N>2$ were studied for a chain of harmonically attracting RTPs, for which the mean-square displacement of a single RTP as well as the

two-time correlation have been obtained [33,34]. However the stationary distribution has not been studied, and as we see here, already for $N = 2$, it involves hypergeometric functions. These questions are left for future investigations.

Recently, the simple RTP model of a single particle $dx/dt = v_0\sigma(t)$ in Eq. (1) has been generalized to the case $d^n x/dt^n = v_0\sigma(t)$ with any $n > 0$ [35]. For example, the case $n = 2$ would correspond to an undamped particle driven by a random telegraphic force. It would be interesting to see if our method can be extended to study a pair of such interacting undamped RTPs.

ACKNOWLEDGMENT

This research was supported by ANR Grant No. ANR-17-CE30-0027-01 RaMaTraF.

APPENDIX: DETAILS FOR TWO RTPS WITH DIFFUSION

As stated in the text the stationary solution $\partial_t P_{\sigma_1,\sigma_2}(y) = 0$ of the FP Eq. (36) which obeys (i) continuity at $y = 0$ and (ii) the matching condition Eq. (37) for derivatives has the form

$$P_{\sigma_1,\sigma_2}(y) = \{[b_1 V^1_{\sigma_1,\sigma_2} + b_2 V^2_{\sigma_1,\sigma_2}(\mu_2)]\theta(y) + [b'_1 V^1_{\sigma_1,\sigma_2} + b'_2 V^2_{\sigma_1,\sigma_2}(-\mu_2)]\theta(-y)\}e^{-\mu_2|y|} + [b_3 V^3_{\sigma_1,\sigma_2}(\mu_3)\theta(y) + b'_3 V^3_{\sigma_1,\sigma_2}(-\mu_3)\theta(-y)]e^{-\mu_3|y|} + [b_4 V^4_{\sigma_1,\sigma_2}(\mu_4)\theta(y) + b'_4 V^4_{\sigma_1,\sigma_2}(-\mu_4)\theta(-y)]e^{-\mu_4|y|}, \quad \text{(A1)}$$

where the eigenvectors $\hat{O} = [V^1, V^2(\mu), V^3(\mu), V^4(\mu)]$ are given (in column form) in Eq. (21) and depend on μ via c and s. The parameter μ_2 is given in Eq. (46) and the parameters μ_3, μ_4 are solutions of Eq. (47) and given explicitly in Eqs. (55)–(57). We will now determine the unknown coefficients b_1, b_2, b_3, b_4 and b'_1, b'_2, b'_3, b'_4 from the above conditions (i) and (ii) that we rewrite explicitly. The first one (i) is the continuity condition

$$b_1 V^1_{\sigma_1,\sigma_2} + b_2 V^2_{\sigma_1,\sigma_2}(\mu_2) + b_3 V^3_{\sigma_1,\sigma_2}(\mu_3) + b_4 V^4_{\sigma_1,\sigma_2}(\mu_4) = b'_1 V^1_{\sigma_1,\sigma_2} + b'_2 V^2_{\sigma_1,\sigma_2}(-\mu_2) + b'_3 V^3_{\sigma_1,\sigma_2}(-\mu_3) + b'_4 V^4_{\sigma_1,\sigma_2}(-\mu_4), \quad \text{(A2)}$$

and the second one (ii) is the matching of the derivatives, which reads

$$\mu_2[b_1 V^1_{\sigma_1,\sigma_2} + b_2 V^2_{\sigma_1,\sigma_2}(\mu_2) + b'_1 V^1_{\sigma_1,\sigma_2} + b'_2 V^2_{\sigma_1,\sigma_2}(-\mu_2)] + \mu_3[b_3 V^3_{\sigma_1,\sigma_2}(\mu_3) + b'_3 V^3_{\sigma_1,\sigma_2}(-\mu_3)] + \mu_4[b_4 V^4_{\sigma_1,\sigma_2}(\mu_4) + b'_4 V^4_{\sigma_1,\sigma_2}(-\mu_4)] = 2\frac{\bar{c}}{D} \times [b_1 V^1_{\sigma_1,\sigma_2} + b_2 V^2_{\sigma_1,\sigma_2}(\mu_2) + b_3 V^3_{\sigma_1,\sigma_2}(\mu_3) + b_4 V^4_{\sigma_1,\sigma_2}(\mu_4)]. \quad \text{(A3)}$$

Finally, we will also use that the total probability is normalized to unity. We note that $V^1_{\sigma_1,\sigma_2}$ is orthogonal to all the other vectors for any value of μ. We can thus take the scalar product of all equations with V^1 and obtain

$$b_1 = b'_1, \quad \mu_2(b_1 + b'_1) = 2\frac{\bar{c}}{D} b_1 \Longleftrightarrow b_1 = b'_1 = 0, \quad \text{(A4)}$$

as soon as $\gamma > 0$, which is similar to our result for $p_2 = P_{++} - P_{--} = 0$ in the case $D = 0$, see Eq. (92).

Based on some numerical observation, we now assume that

$$b'_2 = -b_2, \quad b'_3 = b_3, \quad b'_4 = b_4, \quad \text{(A5)}$$

and we will verify below that it indeed provides a solution to the problem. These identities imply from Eq. (A2) that

$$b_2[V^2_{\sigma_1,\sigma_2}(\mu_2) + V^2_{\sigma_1,\sigma_2}(-\mu_2)] + b_3[V^3_{\sigma_1,\sigma_2}(\mu_3) - V^3_{\sigma_1,\sigma_2}(-\mu_3)] + b_4[V^4_{\sigma_1,\sigma_2}(\mu_4) - V^4_{\sigma_1,\sigma_2}(-\mu_4)] = 0, \quad \text{(A6)}$$

and from Eq. (A3) that

$$\mu_2 b_2[V^2_{\sigma_1,\sigma_2}(\mu_2)] - [V^2_{\sigma_1,\sigma_2}(-\mu_2)] + \mu_3 b_3[V^3_{\sigma_1,\sigma_2}(\mu_3) + V^3_{\sigma_1,\sigma_2}(-\mu_3)] + \mu_4 b_4[V^4_{\sigma_1,\sigma_2}(\mu_4) + V^4_{\sigma_1,\sigma_2}(-\mu_4)] = 2\frac{\bar{c}}{D} \times [b_2 V^2_{\sigma_1,\sigma_2}(\mu_2) + b_3 V^3_{\sigma_1,\sigma_2}(\mu_3) + b_4 V^4_{\sigma_1,\sigma_2}(\mu_4)]. \quad \text{(A7)}$$

Replacing the r.h.s. by half the sum of both sides of Eq. (A2) and using the above relations Eqs. (A4) and (A5) one can rewrite Eq. (A7) as

$$\left(\mu_2 - \frac{\bar{c}}{D}\right) b_2[V^2_{\sigma_1,\sigma_2}(\mu_2)] - [V^2_{\sigma_1,\sigma_2}(-\mu_2)] + \left(\mu_3 - \frac{\bar{c}}{D}\right) b_3[V^3_{\sigma_1,\sigma_2}(\mu_3) + V^3_{\sigma_1,\sigma_2}(-\mu_3)] + \left(\mu_4 - \frac{\bar{c}}{D}\right) b_4[V^4_{\sigma_1,\sigma_2}(\mu_4) + V^4_{\sigma_1,\sigma_2}(-\mu_4)] = 0. \quad \text{(A8)}$$

Let us now express these equations using the explicit forms

$$V^2(\mu_2) = \begin{pmatrix} \frac{c_2}{\sqrt{2}} \\ \frac{s_2}{\sqrt{2}} \\ -\frac{s_2}{\sqrt{2}} \\ \frac{c_2}{\sqrt{2}} \end{pmatrix}, \quad V^3(\mu_3) = \begin{pmatrix} \frac{s_3}{2} \\ -\frac{1}{2}(1 + c_3) \\ -\frac{1}{2}(1 - c_3) \\ \frac{s_3}{2} \end{pmatrix}, \quad V^4(\mu_4) = \begin{pmatrix} \frac{s_4}{2} \\ \frac{1}{2}(1 - c_4) \\ \frac{1}{2}(1 + c_4) \\ \frac{s_4}{2} \end{pmatrix}, \quad \text{(A9)}$$

where, for $j = 2, 3, 4$, one has

$$c_j = \frac{-\mu_j v_0}{\sqrt{\gamma^2 + \mu_j^2 v_0^2}}, \quad s_j = \frac{\gamma}{\sqrt{\gamma^2 + \mu_j^2 v_0^2}}, \tag{A10}$$

and $V^j(-\mu_j)$ obeys the same Eq. (A9) with $c_j \to -c_j$ and $s_j \to s_j$. Inserting these expressions for $V^j(\pm\mu_j)$ into Eq. (A6) we obtain only one independent equation,

$$b_3 c_3 + b_4 c_4 = \sqrt{2} b_2 s_2. \tag{A11}$$

Similarly, inserting them into Eq. (A8) we obtain only two independent equations

$$b_4\Big(\frac{\bar{c}}{D} - \mu_4\Big) = b_3\Big(\frac{\bar{c}}{D} - \mu_3\Big), \tag{A12}$$

$$\sqrt{2} b_2 c_2\Big(\frac{\bar{c}}{D} - \mu_2\Big) + b_3 s_3\Big(\frac{\bar{c}}{D} - \mu_3\Big) + b_4 s_4\Big(\frac{\bar{c}}{D} - \mu_4\Big) = 0. \tag{A13}$$

Equations (A11) and (A12) give

$$b_3 = \sqrt{2} b_2 \tilde{b}_3, \quad b_4 = \sqrt{2} b_2 \tilde{b}_4, \tag{A14}$$

$$\tilde{b}_3 = \frac{s_2(\bar{c} - D\mu_4)}{(c_3 + c_4)\bar{c} - D(c_4\mu_3 + c_3\mu_4)}, \quad \tilde{b}_4 = \frac{s_2(\bar{c} - D\mu_3)}{(c_3 + c_4)\bar{c} - D(c_4\mu_3 + c_3\mu_4)}, \tag{A15}$$

in which case we have checked that the third Eq. (A13) is automatically satisfied.

Putting everything together we find that the stationary measure is

$$\begin{aligned} P_{\sigma_1,\sigma_2}(y) = b_2\big\{&\big[V^2_{\sigma_1,\sigma_2}(\mu_2)\theta(y) - V^2_{\sigma_1,\sigma_2}(-\mu_2)\theta(-y)\big]e^{-\mu_2|y|} + \tilde{b}_3\sqrt{2}\big[V^3_{\sigma_1,\sigma_2}(\mu_3)\theta(y) + V^3_{\sigma_1,\sigma_2}(-\mu_3)\theta(-y)\big]e^{-\mu_3|y|} \\ &+ \tilde{b}_4\sqrt{2}\big[V^4_{\sigma_1,\sigma_2}(\mu_4)\theta(y) + V^4_{\sigma_1,\sigma_2}(-\mu_4)\theta(-y)\big]e^{-\mu_4|y|}\big\}, \end{aligned} \tag{A16}$$

where $\tilde{b}_3, \tilde{b}_4$ are given in Eq. (A14) and there remains a single unknown parameter b_2 which is obtained by normalization. Let us thus study the total probability $P(y) = \sum_{\sigma_1,\sigma_2} P_{\sigma_1,\sigma_2}(y)$. One has, from Eq. (A9),

$$\sum_{\sigma_1,\sigma_2} V^2_{\sigma_1,\sigma_2}(\pm\mu_2) = \pm\sqrt{2} c_2, \quad \sum_{\sigma_1,\sigma_2} V^3_{\sigma_1,\sigma_2}(\pm\mu_3) = s_3 - 1, \quad \sum_{\sigma_1,\sigma_2} V^4_{\sigma_1,\sigma_2}(\pm\mu_4) = s_4 + 1. \tag{A17}$$

From Eq. (A16) we thus obtain

$$P(y) = b_2\sqrt{2}[c_2 e^{-\mu_2|y|} + \tilde{b}_3(s_3 - 1)e^{-\mu_3|y|} + \tilde{b}_4(s_4 + 1)e^{-\mu_4|y|}], \tag{A18}$$

and the normalization condition $\int_{-\infty}^{+\infty} P(y)dy = 1$ leads to the following result for b_2:

$$b_2 = \frac{1}{\sqrt{2}\big[c_2 \frac{2}{\mu_2} + \tilde{b}_3(s_3 - 1)\frac{2}{\mu_3} + \tilde{b}_4(s_4 + 1)\frac{2}{\mu_4}\big]}. \tag{A19}$$

Solving for b_2 and inserting into Eq. (A18) we obtain the result for $P(y)$ given in the text in Eq. (60). Substituting into Eq. (A16) gives the complete result for all components of the stationary probability $P_{\sigma_1,\sigma_2}(y)$.

[1] M. C. Marchetti, J. F. Joanny, S. Ramaswamy, T. B. Liverpool, J. Prost, M. Rao, and R. A. Simha, Rev. Mod. Phys. **85**, 1143 (2013).

[2] C. Bechinger, R. Di Leonardo, H. Löwen, C. Reichhardt, G. Volpe, and G. Volpe, Rev. Mod. Phys. **88**, 045006 (2016).

[3] S. Ramaswamy, J. Stat. Mech. (2017) 054002.

[4] É. Fodor and M. C. Marchetti, Physica A **504**, 106 (2018).

[5] H. C. Berg, *E. Coli in Motion* (Springer Verlag, Heidelberg, Germany, 2004).

[6] M. E. Cates, Rep. Prog. Phys. **75**, 042601 (2012).

[7] J. Tailleur and M. E. Cates, Phys. Rev. Lett. **100**, 218103 (2008).

[8] M. Kac, Rocky Mt. J. Math. **4**, 497 (1974).

[9] E. Orsingher, Stoch. Process. Their Appl. **34**, 49 (1990).

[10] G. H. Weiss, Physica A **311**, 381 (2002).

[11] P. Hänggi and P. Jung, Adv. Chem. Phys. **89**, 239 (1995).

[12] J. Masoliver and K. Lindenberg, Eur. Phys. J. B **90**, 107 (2017).

[13] K. Malakar, V. Jemseena, A. Kundu, K. V. Kumar, S. Sabhapandit, S. N. Majumdar, S. Redner, and A. Dhar, J. Stat. Mech. (2018) 043215.

[14] A. P. Solon, Y. Fily, A. Baskaran, M. E. Cates, Y. Kafri, M. Kardar, and J. Tailleur, Nat. Phys. **11**, 673 (2015).

[15] S. C. Takatori, R. De Dier, J. Vermant, and J. F. Brady, Nat. Commun. **7**, 10694 (2016).

[16] A. Dhar, A. Kundu, S. N. Majumdar, S. Sabhapandit, and G. Schehr, Phys. Rev. E **99**, 032132 (2019).

[17] U. Basu, S. N. Majumdar, A. Rosso, and G. Schehr, Phys. Rev. E **100**, 062116 (2019).
[18] O. Dauchot and V. Démery, Phys. Rev. Lett. **122**, 068002 (2019).
[19] U. Basu, S. N. Majumdar, A. Rosso, S. Sabhapandit, and G. Schehr, J. Phys. A: Math. Theor. **53**, 09LT01 (2020).
[20] P. Le Doussal, S. N. Majumdar, and G. Schehr, Europhys. Lett. **130**, 40002 (2020).
[21] A. B. Slowman, M. R. Evans, and R. A. Blythe, Phys. Rev. Lett. **116**, 218101 (2016).
[22] A. B. Slowman, M. R. Evans, and R. A. Blythe, J. Phys. A: Math. Theor. **50**, 375601 (2017).
[23] E. Mallmin, R. A. Blythe, and M. R. Evans, J. Stat. Mech. (2019) 013204.
[24] A. Das, A. Dhar, and A. Kundu, J. Phys. A: Math. Theor. **53**, 345003 (2020).
[25] P. Le Doussal, S. N. Majumdar, and G. Schehr, Phys. Rev. E **100**, 012113 (2019).
[26] O. Bénichou, C. Loverdo, M. Moreau, R Voituriez, Rev. Mod. Phys. **83**, 81 (2011).
[27] P. G. de Gennes, J. Stat. Phys. **119**, 953 (2005).
[28] H. Touchette, E. Van der Straeten and W. Just, J. Phys A: Math. Theor. **43**, 445002 (2010).
[29] R. J. Martin, M. J. Kearney, and R. V. Craster, J. Phys. A **52**, 134001 (2019).
[30] S. Sabhapandit and S. N. Majumdar, Phys. Rev. Lett. **125**, 200601 (2020).
[31] https://en.wikipedia.org/wiki/Cubic_equation.
[32] I. Santra, U. Basu, and S. Sabhapandit, Phys. Rev. E **101**, 062120 (2020).
[33] P. Singh and A. Kundu, J. Phys. A: Math. Theor. **54**, 305001 (2021).
[34] S. Put, J. Berx, and Carlo Vanderzande, J. Stat. Mech. (2019) 123205.
[35] D. S. Dean, S. N. Majumdar, and H. Schawe, Phys. Rev. E **103**, 012130 (2021).